*Review*

# Conductive Textiles for Signal Sensing and Technical Applications

**Md. Golam Sarower Rayhan** [1], **M. Khalid Hasan Khan** [2], **Mahfuza Tahsin Shoily** [3], **Habibur Rahman** [2],
**Md. Rakibur Rahman** [3], **Md. Tusar Akon** [3], **Mahfuzul Hoque** [3], **Md. Rayhan Khan** [2], **Tanvir Rayhan Rifat** [3],
**Fahmida Akter Tisha** [3], **Ibrahim Hossain Sumon** [4], **Abdul Wahab Fahim** [4], **Mohammad Abbas Uddin** [3,*]
**and Abu Sadat Muhammad Sayem** [5,*]

[1] Department of Textile Engineering Management, Bangladesh University of Textiles, Dhaka 1208, Bangladesh
[2] Department of Yarn Engineering, Bangladesh University of Textiles, Dhaka 1208, Bangladesh
[3] Department of Dyes and Chemical Engineering, Bangladesh University of Textiles, Dhaka 1208, Bangladesh
[4] Department of Apparel Engineering, Bangladesh University of Textiles, Dhaka 1208, Bangladesh
[5] Manchester Fashion Institute, Manchester Metropolitan University, Manchester M15 6BG, UK
* Correspondence: abbas.shiyak@dce.butex.edu.bd (M.A.U.); asm.sayem@mmu.ac.uk (A.S.M.S.)

**Abstract:** Conductive textiles have found notable applications as electrodes and sensors capable of detecting biosignals like the electrocardiogram (ECG), electrogastrogram (EGG), electroencephalogram (EEG), and electromyogram (EMG), etc; other applications include electromagnetic shielding, supercapacitors, and soft robotics. There are several classes of materials that impart conductivity, including polymers, metals, and non-metals. The most significant materials are Polypyrrole (PPy), Polyaniline (PANI), Poly(3,4-ethylenedioxythiophene) (PEDOT), carbon, and metallic nanoparticles. The processes of making conductive textiles include various deposition methods, polymerization, coating, and printing. The parameters, such as conductivity and electromagnetic shielding, are prerequisites that set the benchmark for the performance of conductive textile materials. This review paper focuses on the raw materials that are used for conductive textiles, various approaches that impart conductivity, the fabrication of conductive materials, testing methods of electrical parameters, and key technical applications, challenges, and future potential.

**Keywords:** e-textiles; smart textiles; conductive polymers; conductive textile testing

## 1. Introduction

Textiles with functional properties such as antimicrobial efficacy, water repellency, and fire retardancy have been known for decades. Similarly, when conductive properties are imparted to textiles, their applications go beyond many known traditional uses. Conductive textiles can be used to devise electrodes and sensors to capture signals, shield against electromagnetic waves, and harvest energy [1]. The earliest known use of wearable conductive textiles dates back to 1883 when conductive headbands were worn by the "La Farandole" ballet dancers [2]. Since then, their application areas have gradually expanded to different domains thanks to the advances in material science and engineering and information technology [3]. Conductive textiles have been recognized profoundly during the last two decades due to some outstanding characteristics, such as their flexibility, lightweight structure, wide range of conductivity, adaptability with the human body, adequate mechanical and chemical durability, and expanded life cycle [4,5].

An increasing number of research studies reported in the scientific literature illustrate the significant interest in conductive textiles [6]. Several books have been published reviewing conductive materials and the recent applications of conductive textiles [7,8]. Still, a combined review on conductive materials and fabrication processes of conductive textiles remains as a literature gap. The aim of this review is to provide a comprehensive understanding of the key conductive materials and pathways for developing and testing conductive textiles. Some important technical applications of conductive textiles, such as electromagnetic shielding, supercapacitors, soft robotics, and e-textiles are overviewed.

## 2. Materials Used to Impart Conductivity on Textiles

Textiles can be given conductive features by using three types of materials: (a) conductive polymers, (b) conductive metals, and (c) conductive non-metals. These are explored in detail in the following subsections.

### 2.1. Conductive Polymers

Electroconductive polymers are organic polymers that retain conductivity over a wide range of magnitudes based on the doping mechanism and bond-conjugated system in their polymeric structures. These polymers combine the beneficial characteristics of typical polymers and metals [9]. The most used conductive polymers are Polypyrrole (PPy), Polyaniline (PANI), and Poly(3,4-ethylenedioxythiophene) (PEDOT), and their chemical structures are given in Figure 1 with descriptions afterward.
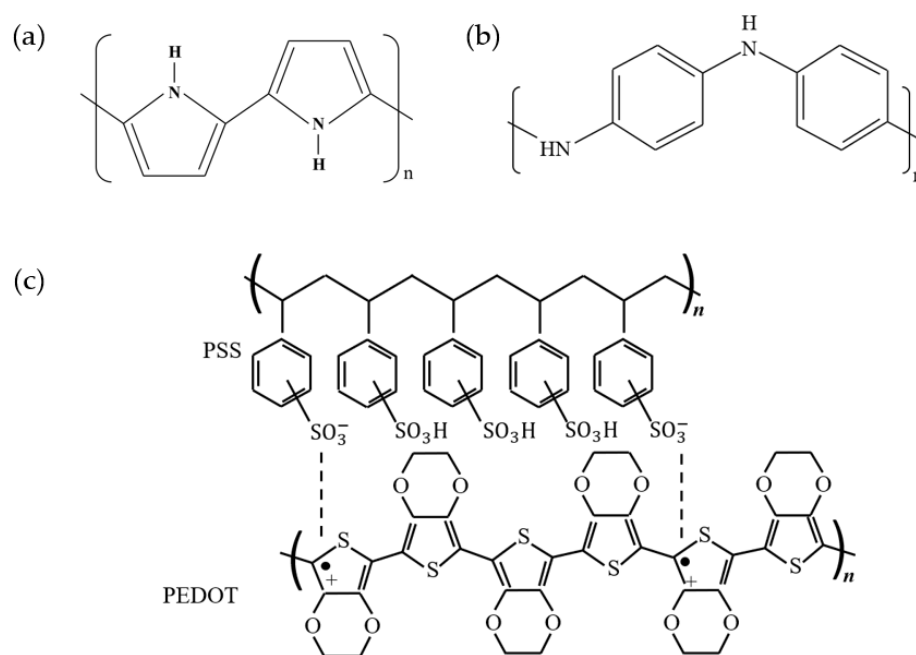


**Figure 1.** Chemical structure of most conductive polymers: (**a**) Polypyrrole (PPy), (**b**) Polyaniline (PANI), (**c**) Poly(3,4-ethylenedioxythiophene) (PEDOT) [10–12].

### 2.1.1. Polypyrrole (PPy)

PPy is one of the most extensively studied conducting polymers for many commercial applications due to their excellent thermal stability, good electrical conductivity, relative ease of synthesis, and environmental stability [10,13]. Three different methods of polymerization of pyrrole are usually followed to obtain PP; These methods are: (i) chemical polymerization in solution, (ii) chemical vapor deposition (CVD), and (iii) electrochemical polymerization [14].

Electroconductive PPy can be prepared in various solutions such as water, diethyl ether, and acetonitrile (ACN). PPy powder prepared in $H_2O$ exhibits the largest capacitance value, approximately 355 $Fg^{-1}$ [15]. The preparation of conducting membranes by chemical polymerization of PPy in the pores of the macroporous membrane in a similar way was also reported. The conductivities of the order of $10^{-3}$ $Scm^{-1}$ and $10^{-2}$ $Scm^{-1}$ were obtained, indicating that thinner composites with a more homogenous distribution of PPy throughout the sample performed better compared to the thicker composites [16]. Chemical polymerization of PPy on the surface of a porous graphite fiber matrix was done to prepare composite electrodes for supercapacitors. A specific capacitance of about 400 $Fg^{-1}$ and a coulombic efficiency of 96–99% were obtained in the presence of ferric nitrate $(Fe(NO_3)_3.H_2O)$, along with indicating that the dipping method is suitable for

the modification of carbon-based porous graphite fibers to improve the performance of electrodes used in supercapacitors [17].

Single-walled carbon nanotube (SWCNT)-PPy nanocomposite electrodes were fabricated to improve the specific capacitance of the supercapacitor. A high specific capacitance was reported compared to the pure PPy and the SWCNTs. The SWCNT-PPy nanocomposite electrodes show a maximum specific capacitance of 265 $Fg^{-1}$ [18]. Similarly, to improve the conductivity of the PPy compared to its pure form, an SWCNT-PPy was prepared by in situ chemical polymerization [19]. PPy-coated multi-walled carbon nanotubes (MWCNTs) prepared by the in situ chemical polymerization of pyrrole showed improved conductivity compared to pure PPy. The room temperature electrical conductivity of the MWCNT-PPy nanotubes synthesized by the chemical method using $FeCl_3$ was measured to be 1.50–2.40 $Scm^{-1}$, which is higher than that of PPy and neat MWCNT. The conductivity decreases with the increase of the feeding mass ratio of PPy to MWCNTs [20].

### 2.1.2. Polyaniline (PANI)

PANI has become an influential resource for conductive textiles because of its facile manufacturing techniques, biocompatibility [21], porous nature [22], thermal stability up to 420 °C [23], catalytic behavior [24], distinct adaptation methods for acquiring diversified behavior, various colorful forms and their interconversion [25], and its transparent medium [26]. Although the application of PANI was initially for use as writing ink, it was first acknowledged by Marcel Jozefowicz with his research group (researchers of the School of Industrial Physics and Chemistry of the City of Paris) as an electroconductive material during the late 1960s [7]. The polymer molecules of PANI are incorporated with poly-conjugated chains derived from reversible phenyl rings and nitrogen-based groups. The profound delocalization, polarization, and one-dimensional characteristics of $\pi$-electron clouds of poly-conjugated networks have led to the outstanding structural, optical, and electroconductive dispositions of PANI.

Numerous versatile polymerization techniques, such as oxidative polymerization, direct and inverse emulsion polymerization, interfacial polymerization, solution polymerization, seeding polymerization, metathesis polymerization, and self-assembling polymerization, have been adapted to synthesize PANI [27]. Customarily, three forms of PANI, exhibited in Figure 2, can prevail, thereby relying on their extent of oxidation and degree of protonation. These are:

(a). Leucoemeraldine $(C_6H_4NH)_n$—100% reduction level
(b). Emeraldine $([C_6H_4NH]_2[C_6H_4N]_2)_n$—50% oxidation, 50% reduction
(c). Pernigraniline $(C_6H_4N)_n$—100% oxidation level

Only the Emeraldine form of PANI can be applied directly to the textiles to impart conductivity among these three categories; however, the pristine emeraldine retains a lower conductivity level and limited processability [25].
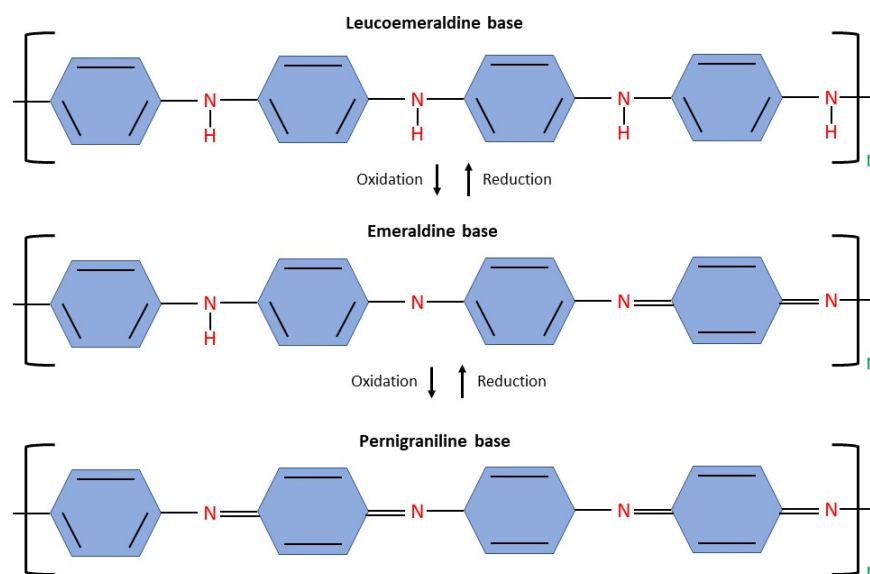
**Figure 2.** Chemical structure of different forms of PANI, adapted from [28] following Creative Common Licence.

Though the potential growth of PANI-based conductive textiles has escalated drastically in recent years, the inherent toxic nature and lower conductivity of PANI than metallic particles, even compared to other intrinsic conductive polymers (PEDOT, PPy) are still the major handicaps for commercializing PANI-based conductive materials. Notable research projects related to ascertaining the environmentally friendly and cost-effective synthesis process of PANI-based conductive textiles have been reported [29,30].

### 2.1.3. Poly(3,4-ethylenedioxythiophene) (PEDOT)

PEDOT demonstrates an intrinsic electroconductive polymer that incorporates two linked groups of benzene rings where two carbon atoms of each are substituted by oxygen atoms and a sulfur-based pentagonal thiophene ring. PEDOT can be easily synthesized from a 3,4-ethylenedioxythiophene (EDOT) monomer through oxidative [31] and electrochemical [32] vapor phase polymerization (VPP) techniques [33], but it cannot be executed commercially due to its lower dispersion in water. As a result, a template polymer poly (styrene sulfonate) (PSS) is utilized during the synthesis of PEDOT, which yields a water-dispersible and transparent film-like polymer that can be conveniently processable [34].

Uniform dispersion in water, convenient methods to adapt electrical properties, high flexibility, excellent transparency (up to 95%), stability against humid air and high temperature are some of the features that allow PEDOT:PSS to add a new dimension over the other intrinsic polymers in terms of diversified practical applications of conductive textiles, such as solar cells [35], electricity storage devices [36], electrochromic devices [37], electrochemical transistors [38], OLED [39], patch antenna [40], supercapacitors [41], actuators [42], and strain sensors [43]. Several variants of PEDOT:PSS dispersions are available according to their molecular weight under the trade name of Clevios and Orgacon given by Heraeus Epurio and Agfa Gevaert, respectively; however, the corrosiveness and unfavorable impacts of PSS cause impediments to the expedition of conductive textiles approach towards the green industry. Studies on the eco-friendly application of conductive PEDOT films on textiles have been reported. Lock et al. experimented with a customized vacuum chamber for the eco-friendly deposition of PEDOT films on the substrates, thereby resulting in conductive substrates that exhibit a noteworthy conductivity of 105 $Scm^{-1}$, including an 84% transmittance of visible light [44]. Brooke et al. applied the VPP technique to synthesize eco-friendly PEDOT: Tosylate films coated with conductive electrodes [45]. Later, Vacuum vapor phase polymerization (VVPP) was acquainted with feasible scale-up production of PEDOT-coated conductive textiles with significant conductivity (1485 $Scm^{-1}$) [46].

Though being one of the most promising conductive polymers, the employment of PEDOT in conductive textiles is limited to research projects and narrow fields of practical application due to its relatively lower conductivity for the proper optimization of PEDOT in wearable electronics; unstable conductivity for any change of temperature, humidity, bending and washing cycles [47]; and maintaining the precise process control parameters during the in situ polymerization of EDOT monomer [7].

Notable works are ongoing to deal with these challenges of PEDOT [48,49]. Until now, the commercial aspects of PEDOT have been fully established in the applications of capacitors, printed wiring boards, packaging films, photographic films, electronic films, and electroluminescent lamps [7].

### 2.2. Conductive Metals

Metals, such as copper, silver, and steel, are the most electroconductive materials, and are extensively used in smart textile applications such as copper yarns and silver-coated fibers [1,50]. Silver (Ag), gold (Au), copper (Cu), titanium dioxide ($TiO_2$), zinc oxide (ZnO), nanolayered clay, and other organic and inorganic nanoparticles and their nanocomposites are applied to textile materials to pass on different multifunctional properties [51]. The conductivity of metallic-nanoparticle-coated threads is low because their small size leads to many interparticle junctions [52].

A few metals and metal-derived oxides used in textile finishing are discussed here.

### 2.2.1. Silver Nanoparticles (AgNPs)

AgNPs are known to be antibacterial, and their therapeutic properties have been proven against a broad range of microorganisms that can cause diseases. Ag can be synthesized through various methods ranging from simple chemical reduction processes to photochemical, biochemical, sonochemical, and Tollens' reagent methods [51]. The deposition of nanowire films around threads can be achieved through dip-coating [52]. Chemically metallized Ag threads are used to produce textiles with antistatic properties or to shield against electromagnetic waves. Ag-coated fibers are used to improve the behavior of smart textiles [50].

### 2.2.2. Gold Nanoparticles (AuNPs)

AuNPs are widely known for their optical and biological properties. They could be used for highly sensitive diagnostic assays, thermal ablation, radiotherapy enhancement, and drug and gene delivery. They are mainly prepared via the chemical reduction method using gold salts such as hydrogen tetrachloroaurate ($HAuCl_4$) as a precursor and citrate as a reducing agent [51]. Au nanoparticles chemically synthesized by citrate reduction can be immobilized onto chitosan-treated soybean knitted fabric via the exhaustion method [53]. A gold coating with solution deposition on knitted fabric is highly conductive, stretchable, wearable, and washable [54].

### 2.2.3. Copper Nanoparticles (CuNPs)

CuNPs have heat transfer properties such as high thermal conductivity, low preparation cost, antibacterial efficiencies, catalytic activity, and electrical and optical properties. They are produced by the chemical reduction method [51]. The surface of the textile fabric can be covered with a layer of densely packed Cu particles after ELD [55]. Cu-coated textiles can show a bactericidal effect [56]. The antibacterial property is important because electromagnetic interference (EMI) shielding fabrics are excellent media for microorganism growth [57].

### 2.2.4. Metal Oxide Nanoparticles (MONPs)

MONPs are renowned for their environmental remediation and electronic applications. The particles can generate charge carriers through energy absorption. $TiO_2$ and ZnO are widely used in textile finishing [51]. Nano-iron oxide, nano-copper oxide, nano-cobalt

oxide, and nano-manganese oxide in cotton fabrics can be created for high antibacterial efficiency. In addition, UV protection and flame retardation can be developed by in situ preparation of nanometal oxides [58].

### *2.3. Conductive Non-Metals*

Carbon-based materials (CNTs, graphene, carbon fibers, carbon aerogels) play a fundamental role in this type of conductive textiles. These materials are characterized by high electroconductivity ($10^4$ Scm$^{-1}$), superior strength, environmental stability, and a cost-effective manufacturing process that exposes these as promising materials for wearable electronics [59]. Many research studies have demonstrated the remarkable features of these non-metallic conductive textiles [60,61]. In recent years, nanocomposites have been intensified for their mechanical, electrical, and thermal performances, where carbon, such as carbon nanofiber, CNTs, graphene, and graphite, are used as a filler [62]. CNTs and graphene have been given special attention due to their unique features, such as their high mechanical stiffness, tensile strength, and exceptional thermal and electrical conductivity [63,64]. Researchers are continuing to discover new dimensions of carbon nanomaterials. After that, a more versatile material, graphene, was discovered and focused on flexibility, higher electron conductivity, and increasing the scope of applications [65].

### 2.3.1. Carbon Nanotube (CNTs)

CNTs are unique nanostructures theoretically considered one-dimensional (1D) quantum wires. The basic building block of the CNTs is very long cylindrical single-walled carbon nanotubes (SWCNTs) that are one atom in wall thickness and ten atoms in circumference. CNTs are the seamless cylindrical shape of graphene sheets. Iijima (a Japanese physicist and inventor) first observed the multi-walled carbon nanotubes (MWCNTs), which were remarkable for their unique structure and electrical properties [66]. After two years, Iijima and his team discovered SWCNTs, which were supposed to be an important material for their theoretical experiment [67]. It was predicted in 1992 that a historical breakthrough would happen in 1996 after successfully synthesizing bundles of aligned single-wall carbon nanotubes with very small diameters [68].

CNTs have many exceptional physical properties. CNTs are 100 times more potent than the highest grades of carbon steel, and their higher tensile modulus can almost be stretched five times the original length [69,70]; moreover, CNTs show extraordinary electronic properties such as $10^2$–$10^6$ Scm$^{-1}$ for SWCNTs and $10^3$–$10^5$ Scm$^{-1}$ for MWCNTs [71], which perform better than copper when transporting electrons long distances without interruption [72,73]. Consequently, it is considered the ideal nanotube because of its mechanical and electrical characteristics. Given this, many potential applications have been proposed, such as H$_2$ storage media [74,75], batteries [76], solar cells [77], transistors [78,79], diodes [80,81], and sensors [82,83].

CNTs have a high aspect ratio that makes them suitable for reinforced materials. CNTs can make pure CNT fiber or reinforce polymeric, ceramic, and metallic fibers. CNT fibers have been processed from aqueous dispersions and dispersions in strong acids, drawn from CNT forests, or pulled from a CNT CVD reactor in the form of an aerogel fiber.

CNTs have shown a great range of variety in applications in the last couple of decades of research. However, with the potential of CNTs, it has gained limited success in the marketplace, especially due to issues in processing and scaleup. There are also intrinsic challenges at the nanoscale (such as assembly, the role of interfaces, and contacts), which also affect the applications' progress. Instead of these challenges, a few applications of nanotubes are available commercially.

### 2.3.2. Graphene

Graphene is a two-dimensional (2D) monolayer [84] ultra-thin carbon film [85] with a hexagonal structure [86] that has become the center of attraction for researchers due to its exceptional electrical conductivity, as well as its thermal, mechanical, optical, and elec-

trochemical properties [87]; moreover, some extra mentionable intrinsic properties added extra advantages when embedded into microstructures, which is crucial for promoting its potentiality in practical uses [88–90]. As a consequence, the development of graphene-based 3D aerogels (GBAs), 2D membranes (GBMs), and 1D fibers (GBFs) have progressed. Three-dimensional GBAs have achieved the current world record as the lightest material, having a density of 0.16 mg cm$^{-3}$ [91]. Two-dimensional GBMs can be produced by CVD or infiltration processes for energy storage and conversion. However, one-dimensional GBFs are more applicable than GBFs and GBMs for their electrical and mechanical properties. GBFs are flexible and fabricable; therefore, they can be used in any form and in multifactional applications. Graphene can be produced in monolayer and multi-layer forms based on the application. The rapid acceptance of graphene as a substance of interest lies in its actual availability in the preparation technique and perhaps mostly because monolayer and multi-layer graphene and graphene oxide (GO) have several versatile properties.

Graphene can be chemically modified to obtain inexpensive materials such as graphene oxide (GO) [92], reduced graphene oxide (rGO) [93], and their derivatives (fGO, frGO and mG) on a large scale. This chemical modification is done to get fibers, films, porous frameworks, or modified or hybridized forms to diversify their function. Graphene-based materials such as GO and rGO have great prospects for use as a material for eco-friendly wearable e-textiles [41,94–97]. The negative charge in GO helps to generate and facilitate their association with the fibers/fabrics' functional groups [98]. Thus, it helps with the better fixation of textile fabrics and of acquiring flexible, washable, and durable wearable e-textiles [99].

As graphene was an extraordinary material for future technologies, great emphasis was given to bulk production [84]. Various bulk production methods have been approached, including the 'Hummers' method for large-scale graphene synthesis [100]. A chemical [101] or thermal [102] reduction process is performed to procure reduced GO. There are also other methods to produce GO by ion implantation, CVD [103], mechanical exfoliation, chemical exfoliation, electrochemical exfoliation, liquid phase exfoliation, and epitaxial growth on silicon carbide (SiC) [104,105], but many of these are not popular. Graphene can be formed with other materials containing special characteristics to get a unique composite material. Nanocomposites such as polymer, active carbon, metal, metal oxide, and carbon fiber are employed with graphene to get exceptional properties. Polymer nanocomposites are generally fabricated using GO and rGO as fillers. Graphene-based nanocomposites can be used as potential applications for energy storage and conversion [106–108], electromagnetic interference shielding [109,110], and sensors [111]. Activated carbon with graphene is advantageous for its wide range of availability and relatively good performance due to its large surface area. Graphene/activated carbon can be used as an electrode (cathode) in Li-ion batteries [112], high-performance supercapacitors [113,114], and sensors. Metals such as Pt, Al, Pd, Co, Si, Mg, Cu, Au, Fe, and Ce have been embodied into graphene as a composite for supercapacitor sensors. Graphene/metal oxide composites are used as capacitive materials for supercapacitors due to their higher density of energy [115].

The potential application of graphene can be for manufacturing high-capacity batteries [116,117], actuators [118–120], supercapacitors [121,122], more efficient solar cells [123,124], corrosion prevention [125], circuit boards [126], and medicinal technologies such as the point-of-care detection of diseases [127], in field-effect transistors [85], transparent electrodes [88,128], energy storage materials [129], composites [130], chemical and biosensing [131,132], and many other areas; so many scientists are focusing on the revolutionary nature of graphene and how it could be commercially utilized into everyday life.

## 3. Fabrication Processes of Conductive Textiles

Fine metal wires can be combined with textile structures during textile processes like spinning, knitting, and weaving, but it may come at the sacrifice of flexibility and the tactile properties of traditional textiles [133]; however, the common alternatives to them are: modifying textile surface by depositing a conductive layer with the help of additional

finishing processes such as a deposition [134]; coatings such as dip coating, spray coating, rod coating, or roller coating on the textile substrate (fiber, yarns, fabrics) [135]; and printing textiles with conductive materials [136]. The choice of the process depends on the process parameters and properties such as flexibility, stability, and degree of conductivity of the final products [59]. The common approaches are described in the following subsections.

### 3.1. Deposition Method

The deposition is an effective way of applying a thin coating on textile substrates. Metals or non-metals and intrinsically conductive polymers (ICPs) can be deposited on a suitable substrate by following three steps: (a) scatter or vapor deposition, (b) employing sol precursor, and (c) sintering the substrate to start a sol-to-gel transformation [137].

#### 3.1.1. Vapor Deposition

Highly pure and high-performing solid materials, such as metal, nanotubes, and ICP, are deposited as thin films of one or several layers [138]. The deposition of thin perovskites is a thin film based on organo-inorganic materials, such as $CH_3NH_3PbX_3$ ($X = I-, Br-, Cl-$), which has fascinating optical and electronic properties [139]. A film of solid and liquid through vapor deposition without solvent has been investigated. In vapor deposition, vapor can be condensed by two processes: (a) physical condensation or (b) chemical reaction; furthermore, depending on these two processes, vapor deposition is classified by: (i) physical vapor deposition (PVD) and (ii) chemical vapor deposition (CVD) [140].

1. Physical Vapor Deposition (PVD)

PVD was developed to address the capacity to create a layer with continuous electrical conductivity and the ability to create an element with a specific geometry and dimensions, which is not possible in conventional layering technology such as printing, dipping, etc. [141]. PVD is a process of applying a fine coating of conductive materials on the textile substrate by the vaporization process. PVD comprises four steps: (a) production of vapor phase by evaporation of target materials, (b) transportation of the vapor to the substrate, (c) reaction between the metal atoms and the appropriate reactive gas, and (d) condensing vapor on the surface of the substrate [51,142,143]. PVD can be deposited in almost all materials, such as pure metal, metal, and organic material mixtures such as glasses, alloys, compounds, and layer systems [144]. Silva et al. studied the PVD of aluminium on bare Kapton and when it was coated with PVC/PU [145]. The PVC-coated substrate was the best among the samples for making flexible electronics. Depending on the deposition technique, PVD can be classified by evaporation techniques (vacuum thermal evaporation, electron beam evaporation, laser beam evaporation, pulsed electron deposition, arc evaporation, molecular beam epitaxy, ion plating evaporation) [146] and the sputtering technique [147–149]. A silver coating was deposited on cotton fabric using PVD (vacuum thermal evaporation) with a Flexicoat 850 coating apparatus to impart conductivity [150]. The same process was used to deposit a nano-coating of Al and Zn on cotton fabric, with Zn coating having a greater EMI shielding performance than Al-coated cotton fabric [151].

Sputtering is a non-thermal physical vapor deposition technique where molecules move from the surface of the material through the knocking of high energy particles. Molecules that emerge from the target material by the shell firing of high energy particles on the material are condensed on the surface of the substrate to deposit a thin film of the target material [152]. Park et al. investigated DC magnetron sputtering of an Ni-Fe/Cu multi-layer (500 nm Ni-Fe/500 nm Cu) thin film to impart conductivity and led to an EMI shielding effect in the range of 0.7 GHz–6 GHz, which is a better EMI shielding effect than a pure Ni-Fe and Cu layer [153]. Sputtering deposition of Cu metal is used to make ECG electrodes for biomonitoring smart wear [154]. Wang et al. reported the very first PVD of amorphous carbon-coated 3D $NiCo_2O_4$ on carbon cloth to make a binder-free flexible electrode with high dimensional and cyclic stability (535.47 $mAhm^{-1}$ at 500 mA $g^{-1}$ for 100 cycles) capacity and electrochemical performances [155]. A better electrochemical performance was found for $NiCo_2O_4/NiO/C$ composites on carbon cloth obtained by

magnetron sputtering PVD of $NiCo_2O_4$ nanowires/NiO nanoflakes with cyclic stability (1051 mAh $g^{-1}$ for 100 cycles at 100 mA $g^{-1}$) [156].

2.  Chemical Vapor Deposition (CVD)

CVD refers to the segregation or chemical reactions of gaseous reactants near a heated substrate surface in an activated situation (heat, light, plasma), which will finally form a stable solid product [157]. Its history goes back to 1893 when De Lodyguine (an electrical engineer and inventor) deposited tungsten onto carbon lamp filaments through the reduction of tungsten hexachloride ($WCl_6$) by hydrogen ($H_2$). This initiated the pedestal of the industrial utilization of CVD [158]. Typically, the CVD method is applied to deposit conductive polymers on the textile substrate (fiber, yarn, fabric) [159]. The fundamental concept of CVD is a chemical reaction that forms a layer on the substrate from the vapor of the reagents, leaving the by-products in a volatile form.

Researchers experiment with different kinds of materials by using the CVD method to make textile materials conductive. $FeCl_3$-coated cotton yarns were exposed to pyrrole vapor, thereby producing a coated layer of PPy on cotton yarns [160]. The CVD method is adopted for PPy deposition in various fabrics such as viscose, cupro, lyocell, nylon, PET, etc. [161–163].

The CVD process is a recognized technique for making highly conductive polymeric layers on different substrates [164]. To get high conductivity and a uniform polymeric layer on a flexible and rigid substrate, a novel method called Oxidative Chemical Vapor Deposition (OCVD) was implemented [165]. OCVD is a solvent-free technique that results in more homogenous, thin, and highly conductive polymer layers on different substrates. The steps for OCVD of PEDOT include: (i) First, fiber penetration with oxidant ($FeCl_3$) solution and sub-drying; (ii) then, oxidant-enriched fibers were exposed to EDOT monomer vapor; and last, (iii) PEDOT-coated fiber doping. It is reported that the CVD technique could successfully coat PET fabrics with PEDOT, but PEDOT-coated PET fabrics showed reduced conductivity due to poor fiber contact [166]. PEDOT-coated PET yarn fibers with good electrical and mechanical characteristics were developed, which could be converted into woven structures with good electrical properties. Furthermore, viscose yarn was tested in both the CVD and OCVD processes. Although the OCVD process found a high conductivity level of 14.2 $Scm^{-1}$, fewer mechanical properties were obtained at 15 wt% oxidant concentration on viscose yarn [167].

3.1.2. Layer-by-Layer Deposition (LbLD)

LbLD is a new and simple method of developing a thin film on the substrate at normal temperature and pressure. Alternate deposition occurs using a poly-ion layer on solid substrates by dipping into an oppositely charged solution and washing between each depositing layer. The alternation of the surface charge results in polyelectrolytic layers on the solid. Charged particles are bound by the electrostatic and Van der Waals bond [168–171]. The LbLD process has already been applied to impart conductivity to textile materials in many applications [172,173]. Electromagnetic interference shielding of cotton fabric by layer-by-layer (LbL) assembly of positive and negative charge MWCNTs and nickel ferrite ($NiFe_2O_4$) nanoparticles with a PDMS covering to keep the layer stable was reported [169]. A cationic surfactant is employed to create positively charged MWCNT, and EDTA is used to functionalize $NiFe_2O_4$, which is controlled by the ionization of both catalysts [169]. The vacuum-assisted spray-LbLD process can deposit MWCNT without any binder, thereby producing a high degree of binding sites and resulting in better sensing capabilities [174]. Poly(ethylenimine)/CNTs and ammonium polyphosphate layer nanocomposite coating were placed LbL on cotton fabrics to generate superior hydrophobic conductive cotton fabric, and PDMS coating imparted an identical energy density throughout the surface [175]. LbL deposited Chitosan–graphene cation and PSS anion layers one after the other on cotton fabric, resulting in an electrical conductivity of $1.67 \times 10^3$ $Sm^{-1}$ for 10 layers [176]. $V_2O_5$-nanostructured supercapacitors show low energy density and electrical conductivity. Deposition of graphene layers between $V_2O_5$-coated MWCNT films prevents congregation and improves the energy density (96 $Whkg^{-1}$). The graphene layer

acts as a barrier and improves the durability and capacitance of the device [177]. An LbLD process featuring a pad-dry-cure method for developing an electrically conductive Ag nanoparticles–carboxymethyl cellulose composite was reported [178].

### 3.1.3. Electrochemical Deposition

The electrochemical deposition, or the electrodeposition process, is used to deposit (composite/single) thick, stiff coats of conductive materials onto textiles, especially metal particles, with the help of an electric field [179]. In this process, metal ions turn into solid metal and deposit on the cathode surface [180]. Electrochemical deposition has become so popular due to its versatile application for the deposition of different kinds of materials such as metal, metal alloys, composites, nanocoatings [181], ceramic and organo-ceramic materials [182], semiconductors (chalcogenide and oxides) [183], nanocrystalline and nanophase metallic materials [184], graphene-reinforced metal matrices [185], intrinsic conductive polymers (PANI, PPy, PEDOT, PEDOT: PSS) [186], carbon-based materials and their composites (CNTs, graphene, carbon/metal) [187], $MnO_2$–carbon-based materials [188], metal oxides [189], and so on.

Nickel was electrochemically deposited on linen and nylon fabric to produce wearable radar-visible fabrics. Electrodeposition assembly consisted of an electrolyte (nickel sulphate hexahydrate, nickel chloride, Boric acid) cathode and anode. The fabric was connected to the cathode by a platinum strip, and another platinum strip was used as an anode. Electrochemical deposition was done at 4 V for 15 min [190]. The Box–Behnken technique of electroless plating of nickel is reported [191]; they noticed that the deposition amount depended on the time and current applied, and Ni was electrodeposited on the Cu nanowires network to produce a transparent conductive film [192]. A process of targeted electrochemical deposition to produce microelectromechanical devices by employing a non-conductive mask between the anode and cathode and regulating the electrolyte with a pump was proposed [193]. Electroless plating on stretchable fabric aids in electrochemical deposition by providing conductivity to the fabric. Later, the electrochemical deposition of metal on every fiber with conductive material makes the fabric stable and provides optimum conductivity [194]. A simple one-step electrochemical deposition method to produce a metal-organic framework and PPy composite capacitor electrode with the help of dopamine with better conductivity than a virgin metal-organic framework was presented [195]. $MnO_2$-deposited capacitors have low electrical conductivity and have been investigated in many ways to increase this. $MnO_2$ is electrochemically deposited on CNTs to produce pseudo-capacitors [196]. The electrochemical deposition of $MnO_2$ and PPy composite on carbon cloth produced a flexible electrode for supercapacitors with a capacitance of 325 $Fg^{-1}$ and $MnO_2$-coated CNTs deposited on flexible graphene nanosheets produced electrodes for supercapacitors with a capacitance of 442.9 F/g [197]. $MnO_2$ deposited on activated carbon paper improves its capacitance (485.4 F/g) [198]. Kim et al. prepared a flexible photo sensor that deposits ZnO on Ni-Cu-Ni-coated PET fabric and copper deposited on silane molecules, which were polymerized with 2-(methacryloyloxy) ethyl trimethylammonium chloride (METAC)-coated recycled PET nanofibers [199]. Rosa-Ortiz et al. proposed a method of electrochemical deposition with the help of Hydrogen Evolution that improves the speed of copper coating and is directly fused to the wearable fabric, which eliminates the soldering machine [200].

### 3.1.4. Electroless Deposition

Electroless is an elegant and multipurpose process of conductive metal deposition on any surface. Apart from other deposition processes, electroless is an autocatalytic chemical reaction and is done without electrical energy. It can deposit both thickly and thinly coated films quickly and effectively. It can deposit metals such as silver [201], aluminum, copper [202], nickel, and iron, which are uniformly and smoothly deposited on the surface of the textile substrate [51,203]. The main principle uses a reducing agent in a solution for the chemical reduction of metal ions and deposits them on the substrate's surface, which

imparts electrical conductivity to the textile substrate. The chemical reaction involved in this process is as follows [204]:

$$S = S^{n+} + ne^-$$

$$M^{n+} + ne^- = M$$
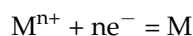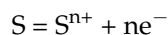
Electroless-deposition-produced conductive textiles, such as conductive woven cellulose fabric [205], PET fabric [206], and others, have a wide range of applications. Silver is deposited with the use of ultrasonics to create a shielding-effective PET fabric [207] treatment with silver nitrate and sodium hydroxide at 130 °C for 1 h, which increases the surface activity and eliminates the need for a catalyst that produces ethylene as a reducing agent, while ammonia treatment stabilizes the conductive layer [208]. Stretchable conductors are prepared by depositing silver through electroless plating on polyurethane filaments [209]. PVC is added to thermoplastic urethane during electroless plating, making the silver layer more adhesive and higher in conductivity.

The electroless deposition of Cu imparts a variety of features to the textile substrates. Cu is seeded with Ag and coated on cellulosic fabric to make it conductive for the manufacture of a light-emitting diode [205]. Lin et al. made ultra-stretchable conductors that deposit Cu on polydopamine-coated cotton fabric with a $Pd^{2+}$ catalyst [210]. Guo et al. employed $AgNO_3$ instead of $PdCl_2$ to deposit Cu on PET textiles, resulting in a more uniform metal distribution and denser layer [211], and hydrazine monohydrate (80 wt%) treatment at 60 °C improved the interaction between PET and the Cu layer [212]. The addition of 3-mercaptopropyltriethoxysilane to PET textiles during a deposition improves the washing performance [213]. Paquin et al. described a three-step copper deposition on cotton using Pd or Ag as a catalyst [214]. Cotton fabric can also be activated by Ag and Cu nanoparticle deposition before the electroless plating of Cu [215]. Cu has been electroless deposited on cotton fabric using $(NH_4)_2PdCl_4$ as a catalyst to create a highly conductive fabric [216]. Laser treatment on cotton fabric improves abrasion resistance [217].

### 3.2. In Situ Polymerization

In recent years, in situ polymerization has become a popular technology for creating conductive nanocomposite because of its varied and advantageous approach to polymerization that directly uses 90 mixtures of monomer and nanoparticles with various additives. Grothe et al. highlighted the differences between in situ polymerization and other surface modification approaches, such as nanoparticle fusing, and the benefits of in situ polymerization over other methods [218]. Due to the intense interaction between two side-by-side polymer chains, most conductive polymers are thermally unstable and not soluble in different solvents. However, in situ polymerization can polymerize in various ways depending on the conductive polymer for different applications, such as in situ chemical polymerization, in situ electrochemical polymerization, in situ vapor phase polymerization, and in situ polymerization in a supercritical fluid [219].

Liu et al. mentioned that in situ polymerization can reduce the impedance of the electrolyte interface and bring interfacial compatibility and stability to solid-state lithium batteries, thereby simplifying the process of polymerization [220]. Highly electrically conductive and thermally stable graphene/polyaniline (GN/PANI) nanocomposite was synthesized by in situ polymerization [221].

In situ polymerization, according to Park et al., aids in the efficient dispersion of carbon SWNTs in polymer composites in the presence of sonication, which was previously challenging due to the non-reactive surface of SWNTs [17]. The resulting nanocomposite is electrically conductive and optically transparent, with improved mechanical characteristics and thermal stability at low concentrations (0.1% of vol). Hong et al. used ferric p-toluenesulfonic acid (FepTS) and $FeCl_3$ as oxidants to investigate in situ polymerization of PEDOT on nylon 6, PET, and poly (trimethylene terephthalate) (PTT) fabrics and compared different properties of PEDOT/nylon-6, which has the best conductivity of all the nanocomposites; however, PTT/PEDOT is the most stable [222].

*3.3. Coating*

A textile conductive coating is a material layer that adheres to a textile structure (fiber, yarn, or fabrics). These coatings are used to make the textile material conductive or to add functionality to the textiles. Coating methods are industrial technologies used to adapt the properties of textiles to those required for technical and specialty applications. The variety of methods allows for good adaption to end-use requirements [223].

3.3.1. Dip Coating

Dip coating is a simple and cost-effective process commonly used in various industrial fields for depositing coating material onto any substrate, along with metallic and ceramic polymer film and textile materials. The process could be interpreted as depositing aqueous liquid phase coating solutions on the surface of any substrate [224–226]. Conductive materials are typically dissolved in solutions that are immediately deposited on the surface of the substrate, after which, to obtain the dry film, the sedimentary conductive wet coating has to be evaporated. The technique associates submerging the textile material in the solution of the conductive coating materials, ensuring that the textile material is completely penetrated and then withdrawn from the solution materials. Notably, this supposedly easy process of constructing film through dip coating comprises complex chemical and physical multi-variable norms. The thickness and morphology of depositing thin conductive films were determined by various criteria such as dipping time, withdrawal speed, dipping cycles, substrate (textile material) surface, density, viscosity, surface tension, and evaporation of the conductive coating solution [227–229]. Various modified dip coating techniques, such as solution dip coating, sol-gel dip coating, multi-layer dip coating, and vacuum-assisted dip coating, are significant to manufacture deposited films on the surface of textile materials.

Solution dip coating is the most straightforward technique of forming a film on textile materials' surfaces and is typically used in increasing production. Since it is the most commonly used method in textile manufacturing, dip coating is often referred to as starch finishing or sizing. Solution dip is a user-friendly process to operate and can increase the efficiency of production. However, on the opposite, the solution of dipping the uniformity of the coating is weak and the bonding state is relatively poor [229]. Cotton fabric containing high electrical conductivity has been confirmed to have been established by a two-step dipping and coating. The cotton fabric was immersed in an acetone solution and rinsed properly with deionized water after drying in an oven. Then, GO was coated onto the fabric surface by dipping the modified cotton fabric into GO dispersed solution for two cycles. After that, a padding process was conducted to remove the excess material using a pair of rollers and high vacuum pressure [230]. The dipping process is shown in Figure 3.
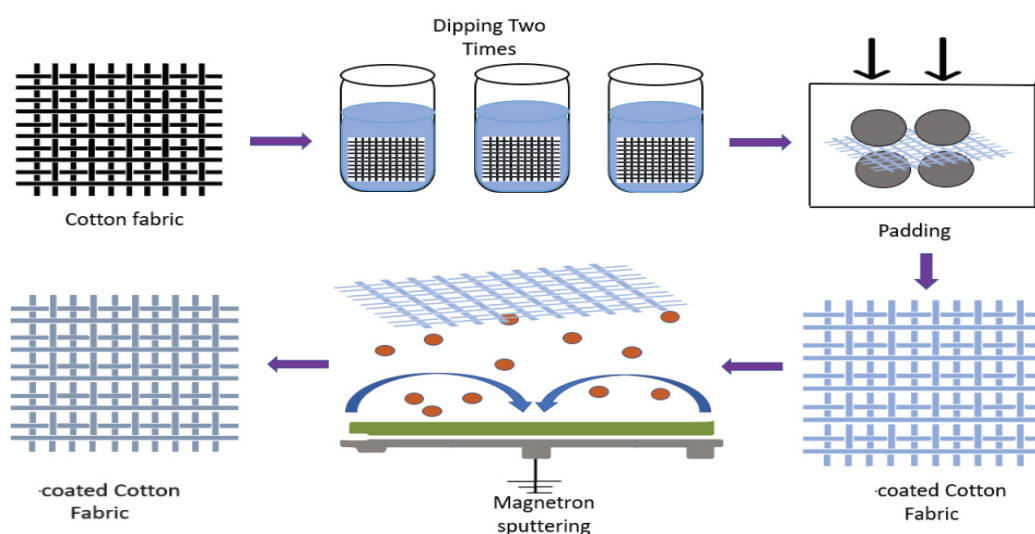


**Figure 3.** The preparation process of silver/graphene-coated cotton fabric, adapted from [230].

Sol-gel technology is a relatively novel method for endowing unique properties upon textiles and is affiliated with decreased ecological impacts [231]. Various functional characteristics such as antibacterial function [232], UV radiation protection [233], dye fastness [234], anti-wrinkle finishing [235], super-hydrophobicity [236], and biomolecule immobilization have been introduced by this method. MWCNTs for conductive purposes and methyltrimethoxy silane for hydrophobicity purposes were coated by the sol-gel process on cotton fabric [237]. The process involves Sol preparation, which is a mixture of methanol, distilled water, and MWCNTs of definite concentration and quantity. Following this, the Sol was mixed well by a magnetic mixer. Then, the cotton fabric was added to the Sol. After checking several parameters, the ultimate result was 40 k$\Omega$ cm$^{-2}$ [237].

To improve the uniformity characteristics or thickness of the single dip coating film, the researchers investigated the multi-layer dip coating. A multi-layer dip coating was studied at a thickness of 90–100 nm and electrical resistance of <400 $\Omega$ mm$^{-1}$ to increase the conductivity of the PEDOT:PSS-coated fibers, and the density and surface tension of the conductive coating solution were varied by altering the mixture ratio, by adding a fluorosurfactant, or by changing the withdrawing speed to achieve a significant, thick PEDOT:PSS layer [238]. Pu et al. organized a two-step dip coating method to establish Ag nanowire networks on the surface of PET materials [239]. The PET substrates were dipped into conductive Ag nanowire solutions and then dried; afterward, the substrate was coordinated vertically to operate the second-step dip coating. The Ag nanowire-coated PET substrates with an order-enhanced analog crisscross structure were prepared. Repeating the multi-layered dip coating method could increase the thickness, improve uniformity, and manufacture the coatings with desired features. Multi-layered dip coating of various coating solutions mainly achieves functional superposition by several deposited films. The fabrication is facile, and it is easy to achieve the multifunctional synergies of each deposited layer. Furthermore, this multi-layer dip coating process benefits broadening the applications of fibrous materials, such as supercapacitors, lithium-ion batteries, and electrode plates.

The vacuum-assisted dip coating method has been introduced to maintain the desired coverage of nanoparticles on the substrate surface with minimal defects, including metallic and ceramic fibers. Liu et al. demonstrated a vacuum-assisted LbL assembly technique to construct electrically conductive substances on textiles to develop multifunctional and flexible textiles with superb EMI shielding performances, super-hydrophobicity, and a highly sensitive humidity response [240]. Cotton fabric was coated with a GO nanosheet via the vacuum filtration deposition method [29]. The woven cotton fabric was treated with sodium hydroxide solution. Vacuum filtration deposition was used to disperse the GO nanosheet aqueous solution into the cotton fabric surface to fabricate GO–cotton fabric. Refluxed graphene and polyvinylidene fluoride (PVDF) were mixed and dissolved in absolute ethanol. This mixture was then forcibly deposited into the cotton fabric via a vacuum filtration deposition process, as shown in Figure 4 [29,241].

The spray coating technique uses a spraying device (found on compressed air, such as with an airbrush or spray gun) to deposit conductive materials on the textile surface by the breeze. Any substrate can be coated by this simple, economic, fast, and scalable process, whether it be round or flat, or flexible or rigid [242]. Recently, it has been published that the spray coating approach that applies PEDOT:PSS conductive materials containing 5 wt% dimethyl sulfoxide (DMSO) made highly conductive and multifunctional PET fabrics. PET fabrics were coated with conductive PEDOT:PSS solutions that contain 5 wt% DMSO via spraying conductive material onto the surface of pre-treated PET fabrics [243].
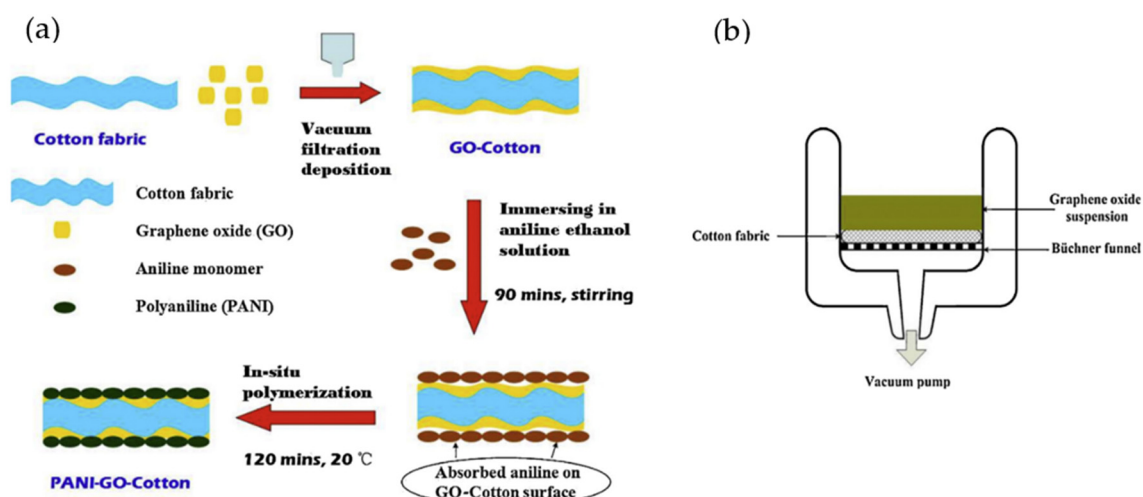
**Figure 4.** Schematic of (**a**) graphene oxide (GO)-coated cotton fabric fabricated by vacuum filtration deposition process, (**b**) PANI-GO-cotton fabric preparation procedure [29] (reprinted with permission from Elsevier).

### 3.3.2. Rod Coating

The rod coating process is easy and inexpensive to penetrate the conductive material on the textile substrate in a continuous and controlled manner (see Figure 5). This technique can affect the uniformity and condition of penetrated thin conductive thin coat by key parameters such as the rod's size, solvents, and conductive solution's viscosity. The concentration of the coating is influenced by the groove size in the wire-wound rod and depends on the rod's diameter. The solution flows through the grooves in the wire-wound rod, resulting in a thin film deposition at room temperature [242]. Zhang et al. reported a simple dry-Mayer-rod-coating method that fabricates the conductive sheath/core-structured graphite/silk fibers and indicates their application as wearable strain sensors [244]. A clip is used to align the bundle of silk fiber at one end of the flat plate. Then, graphite was put on the fixed end of the silk fiber and graphite flakes, which were then moved by a Mayer rod pressed onto the fibers [242].
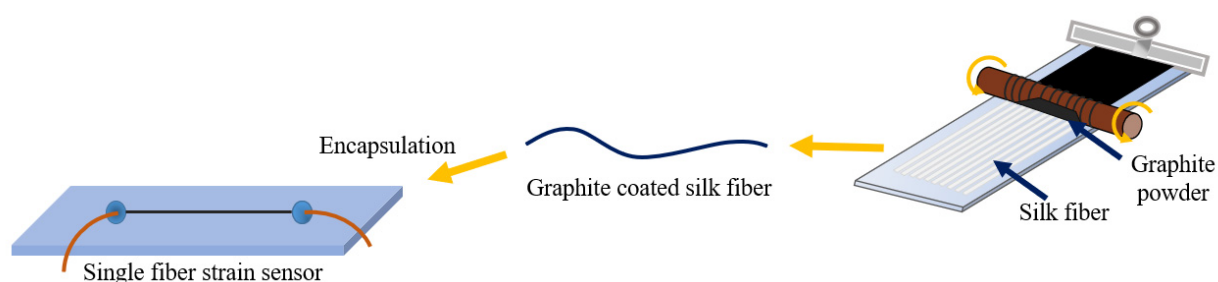


**Figure 5.** Fabrication of sheath/core-structured graphite/silk strain sensor through a dry-Mayer-rod-coating process, adapted from [244].

### 3.3.3. Roller Coating

The Spandex multifilament yarn was coated with thermoplastic polyurethane/carbon nanotube (TPU/CNT) conductive polymer composite (CPC) using the roller coating technique. The conductive mixture was placed into a bath; three rolls pushed the yarn. It was coated when it rolled over the second roll, which was explicitly immersed in the coating bath to pick up the conductive material; next, a glass tube entered with hot air moving through the glass, thereby acting as a drying oven, as shown in Figure 6 [245].

Each coating process has different supremacies that lead to different results. The advantages and disadvantages of various coating processes are shown in Table 1.
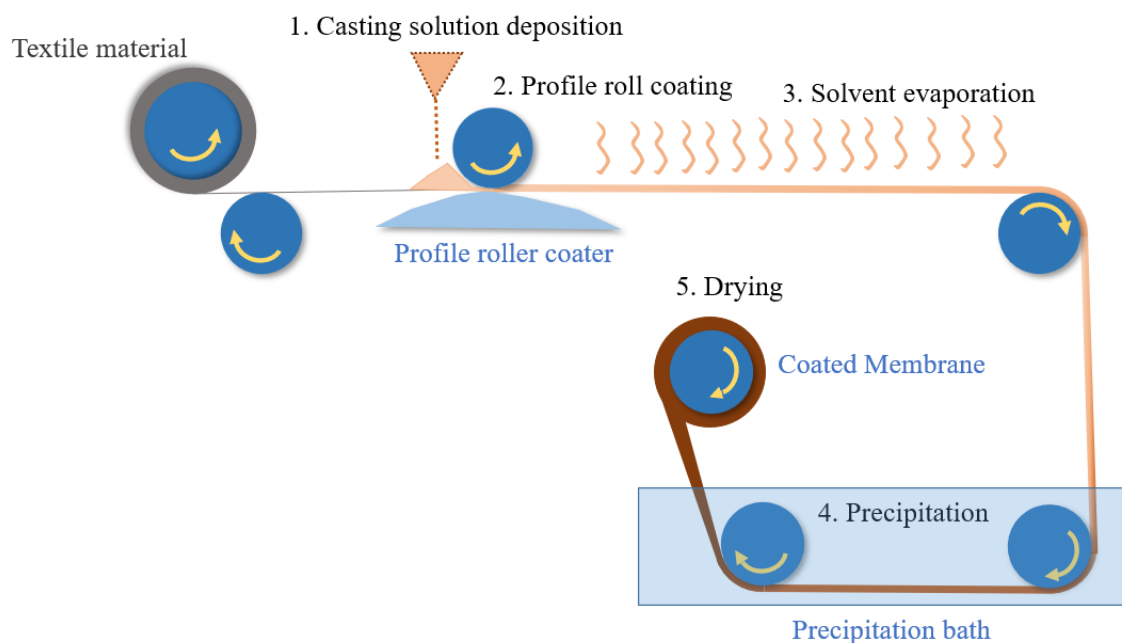
**Figure 6.** Roller coating process.

**Table 1.** Advantages and disadvantages of different kinds of conductive coating processes.

| Processes | Material | Coating Parameters | Advantages | Disadvantages | Ref. |
|---|---|---|---|---|---|
| Directly solution dip coating | Silver/graphene oxide/cotton fabric | Dipping cycle: 2 | user-friendly process | weak uniformity | [230] |
| | | Material to liquor ratio: 1:40 | high efficiency rate | poor bonding state | |
| | | | impressive conductive nature with the least surface resistance of 2.71 ohm/sq. | | |
| | | Gas Pressure: 0.8 Pa | | | |
| Sol-gel dip coating | Organo-silicon/ graphene/ PET fabrics/ polypropylene fabrics | Padding rate: 1 m/min | coated at nearly room temperature | more complex dynamic method | [246] |
| | | Squeezing roll pressure: 15 kg/cm | | harsh chemical reaction on fibrous material | |
| | | Drying temperature: 105 °C | | | |
| | | Drying time: 20 min | | | |
| Multi-layered dip coating | AgNWs/cotton fabrics | Dipping Cycles:1–4 | good uniformity | relative low efficiency | [247] |
| | | | multi-layer structure coating | | |
| Vacuum-assited dip coating | AgNW/MXene/ silk fabric | Dipping time: 1 min | high electrical conductivity (2416.46 Sm$^{-1}$) | | [240] |
| | | Temperature: 50 °C | eco friendly | | |
| | | Dipping Cycles: 10–50 | wide range of substrates | complicated dip coating devices | |
| | | | facilitate coating solution deposition | | |
| Spray coating | PEDOT:PSS/ PET fabrics | Drying temperature: 130 | excellent control over the conductive thickness | isolated droplets | [243] |
| | | | suitable for the deposition of all types of conductive materials | Non-uniform surface | |
| | | Liquid flow rate: 2.5 mL/min | large scale production | | |
| | | Air pressure: 3 bars | | | |
| Rod coating | Graphite/silk fiber | Coating cycles: 10 times | relatively low-cost and highly efficient fabrication of GSF fibers | ineffective with high viscosity liquid. | [244] |
| Roller coating | Thermoplastic Polyurethane (TPU)/CNT/ Spandex Multifilament | Inlet temperature: 200 ± 5 °C | simple and cost-effective process | ineffective with low viscose liquids | [245] |
| | | Dropping temperature: 150 ± 5 °C | continuous process | | [248] |
| | | Roller speed: 0.45 m/min | higher speed | | |

### 3.4. Printing

The printing process is a versatile manufacturing method that enhances and facilitates the field of flexible sensors by providing cost-effective processing routes [249]. Screen and stencil are the two broadly used printing methods for coating conductive materials to different substrates, including textiles [250]. Table 2 presents a comparison of the different printing processes used for fabricating conductive textiles.

**Table 2.** Advantages and disadvantages of different kinds of conductive printing processes.

| Process | Materials | Printing Parameters | Advantages | Disadvantages | Ref. |
|---|---|---|---|---|---|
| Screen printing | CNT/cotton fabrics | • Mesh Density: 300 <br> • Drying temperature: 60 °C | • cheap <br> • good efficient process of forming thick <br> • Good electrical conductivity with a surface resistance of 50.75 Ω/sq | • required high viscosity and low volatile liquid | [251] |
| Inkjet printing | Reactive silver ink/cotton fabric/PET fabric/ wool fabric | • Bitmap:100 dpi <br> • Resolution: 100 steps per inch in the x and y axes <br> • Volume of released drops: ca. 30 nil. <br> • Sintering temperature: 90 °C | • no masking required <br> • low processing temperature based on the drop in demand <br> • high resolution printing <br> • required low viscosity <br> • achieved surface resistance range 0.155–0.235 Ω/sq | • limited printing speed | [252] |
| 3D printing | Ninja flex filament/ PEDOT:PSS/ Polyester fabric | • Extrusion temperature: 230° C <br> • Build Plate Temperature: 30 °C <br> • Printing Speed: 800 mm/min | • no need for molds, dyes, lithographic masks <br> • high efficiency rate | • limited printing material <br> • low printing resolution <br> • poor functionalities | [253,254] |

### 3.4.1. Screen Printing

The first evolution of screen printing dates back to the beginning of the twentieth century. At the time of printing, there was no actual loss of coating solution. The method is shown in Figure 7 and includes a screen of woven material (i.e., synthetic fiber or steel mesh) that has been attached to a tensioned frame. The pattern is generated by filling the screen with an emulsion that is impermeable to the coating solution in regions where no printing can occur. The region of the printed pattern remains open (without emulsion). The screen is then packed with a coating solution and brought close to the substrate. The squeegee is forced to the screen, bringing it into touch with the textile substrate and then linearly drawn across the screen, pushing the conductive coating solution through the open regions onto the textile substrate and thus reproducing the pattern [255].

Screen printing is cheap and is highly efficient in providing thick conductive film [256]. Conductive silver-based inks can be applied to various woven and non-woven textile substances using screen printing to track various vital signs [257]. Sadi et al. have developed a multifunctional weft-knitted cotton fabric through screen printing of CNT ink for wearable electronic devices, smart displays, and cold weather conditioners [251]. There are some difficulties and disadvantages of screen-printed conductive textiles, such as low abrasion resistance and drying out of the ink on the screen, which destroys the design of the screen [249]. The screen printing method is not ideal for single output compared to the direct write printing method [258].
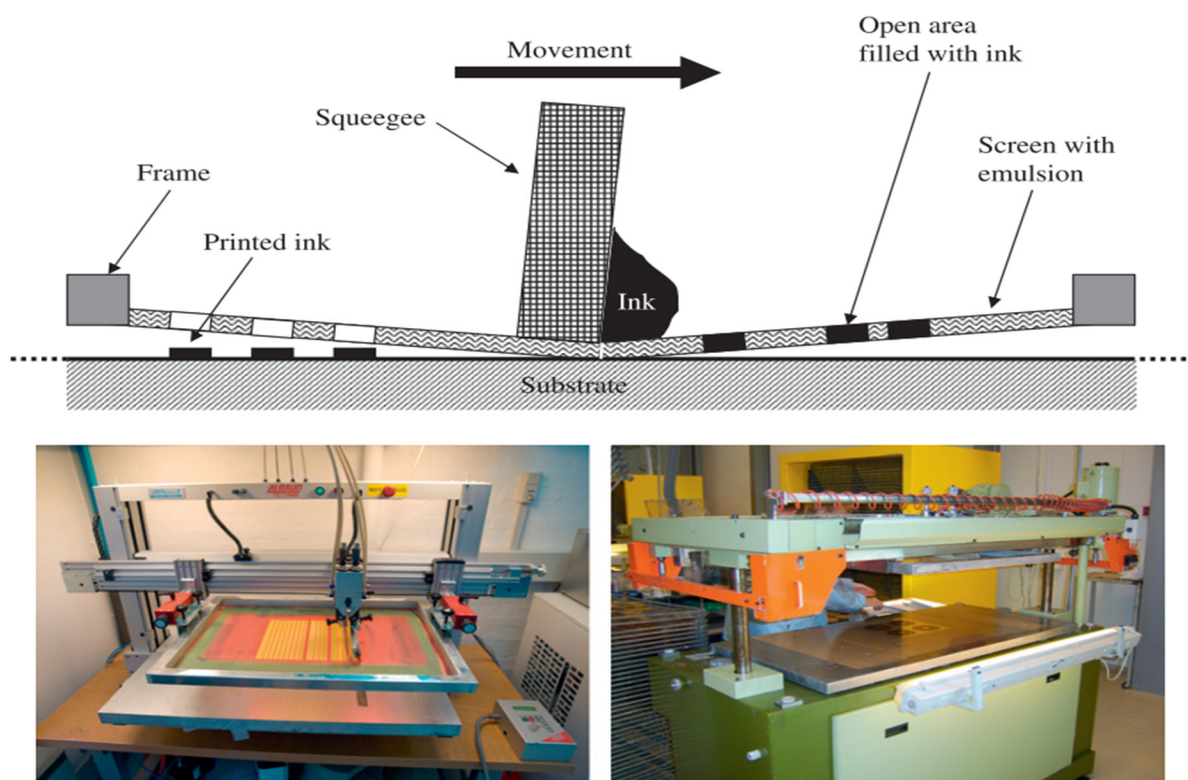
**Figure 7.** Illustration of the screen printing process (**above**) and examples of a laboratory screen printer (**bottom left**) and an industrial screen printer (**bottom right**) [255] (reprinted with permission from Elsevier).

### 3.4.2. Inkjet Printing

Digital or direct printing technology is a way of producing low cost and high quantity conductive materials [259]. Inkjet printing is a way of writing patterns directly to substrates. Inkjet printing is a simple term characterized by dye drops as ink is poured into specific positions to form a printed design on a textile substrate with a specified resolution [260]. In essence, the procedure involves the ejection of a fixed quantity of ink in a liquid-filled chamber in response to applying an external voltage. This abrupt reduction produces a shock wave in the liquid, which induces a drop in the liquid to eject from the nozzle [261]. The expelled drop comes under gravity and air resistance gained in motion, and the surface tension helps slow it along the surface [262]. Then, the drop will dry by solvent evaporation.

Kim et al. developed a knit structure printed with silver inks by inkjet printing, which had a resistance of 0.09 $\Omega$/sq [263]. Low production costs, no masking, non-contact viability, lower material consumption, low temperature, and quick inkjet printing processing have gained interest in cost-effective manufacturing processes [264]. The design can be easily changed as no mask is used [261]. The major advantage of the inkjet printing process is that the conductive material can be deposited only in the required area on the substrate [265].

### 3.4.3. 3D Printing

Three-dimensional printing has gained major importance worldwide for its application in textiles and fashion [266]. Three-dimensional printing techniques have a profound impact on conductive textiles development with multifunctional purposes [267]. Nanocomposites with CNTs or graphene bases possess 3D conductive polymers [268]. The solvent-cast 3D printing method has been characterized by the application of scaffold microstructures (conductive nanocomposite) for its various properties, such as thickness, diameter, and interfilament spacing [269]. Three-dimensional printing of metallic substances enables it to be used for forging stainless steel electrodes with the help of a suitable

laser melting machine and can also perform as a pH sensor [270]. Solvent-evaporation-assisted direct-wire (DW) 3D printing techniques have generated biocompatible polymers comprised of polylactic acid (PLA) and polyethylene adipate (PEA) with barium titanate nanoparticles [268]. The Desktop 3D printing method has also enabled the use of CNTs or graphene as construction materials with electrical and thermal conductivity properties [271]. Boron nitride/polyvinyl alcohol has generated a higher thermal conductivity (1.56 and 2.22) than PVA fabrics and cotton fabrics when fabricated by 3D printing techniques, respectively [272]. The textile substrate can accommodate conductors and antennas with the 3D direct-wire (DW) dispensing method, which can provide more accurate data [273]. As no dye is required in this direct-wire (DW) method, the geometric shapes can be conveniently altered [268].

## 4. Testing for Conductive Textiles

The electrical properties of conductive textile materials require proper characterization based on their applications. They are often characterized through determining the resistance, conductivity, surface resistance or sheet resistance, and EMS (electromagnetic shielding) of the textile substrates. These tests are usually performed following standards or by slightly modifying the standards [134].

### 4.1. Conductivity Testing

The conductivity of textile substrates is mostly measured under a DC power source. Nevertheless, it was inspected that PPy-coated poly-aramid fabrics showed increased conductivity under an AC power source due to an electron hopping charge transport mechanism rather than electron conduction [274–276]. Given this, it is evident that the electrical characteristics may be different for AC-based applications.

The conductivity of polymer coatings is generally determined using the four-probe technique according to the ASTM D-4496 standard. According to the method, four electrical contact terminals are placed in a line at an equal distance on a polymer film. The polymer film is set up on an insulating surface. In this process, a constant current is employed between two outer terminals from a current source, and the voltage is measured between two inner terminals. Conductivity in this method can be calculated from constant current ($I$, ampere) applied to the outer terminals and voltage drop across the inner points ($V$, volt). With sample thickness ($t$), we can measure conductivity following Equation (1). [134].

$$\text{Conductivity, } \sigma = \frac{ln2}{\pi t} \frac{I}{V} \tag{1}$$

The resistance of a fiber or yarn of a specific length can be measured using the four-probe method, two-probe method, multimeters, or by applying the principle of division measurement with a known resistance and unknown resistance (sample). The resistivity value is generally expressed as the resistance per unit length—often in $\Omega cm^{-1}$ or $\Omega m^{-1}$.

According to the two-probe method, two contact points are used. The resistance is calculated by the measured voltage and measured current. The current applied is constant, but a voltage drop over the ammeter limits the measurement's accuracy. In 2010, it was observed that the four-probe technique is suitable for inspecting intrinsic electronic transport properties (behavior of electron transport such as hopping or conduction based on material type), such as metallic nanowires, given that these nanowires may have contact resistance, which cannot be avoided in the two-probe method [277]. Moreover, the four-probe technique is more accurate when the resistance value is small as contact resistance is eradicated.

Surface resistivity, often expressed as square resistance, is the resistance between two points of a fabric or coated surface. It is written as $\Omega$ per square ($\Omega$/sq), and the value is not dependent on the distance between contact points [134]. The AATCC (American Association of Textile Chemists and Colorists) test method 76 is generally exercised to measure the surface resistivity of conductive fabric or surface. The BS 6254:1984 and ASTM

D257-07 test methods can also determine sheet resistance. According to the AATCC test 76, two rectangular-shaped copper plates are placed on a fabric specimen. The resistance (*R*, resistance) between two copper electrodes is measured, or the current (*I*, ampere) is determined by applying DC voltage (*V*, volts). The width (*W*) of the sample and the distance between electrodes (*D*) are also measured. The surface resistivity can be calculated using Equation (2) [134].

$$Rs(\Omega/m) = \frac{W}{D} \cdot R = \frac{W}{D} \cdot \frac{V}{I} \tag{2}$$

The instruments used for these electrical measurements are usually multimeters, voltmeters, and picometers.

### 4.2. Electromagnetic Shielding (EMS) Testing

The EMS effectiveness test is a measurement that determines how a textile substrate performs against electromagnetic interference by weakening it. There is no standardized method to test the EMS of conductive textiles to this day. The following properties or parameters of the textile shielding materials used to manufacture textile assemblies or products for EMI shields are very important to determine [278]:

- Reflection coefficient, which depicts the amount of reflected EM wave under an impedance discontinuity in the transmission medium;
- Absorption coefficient, which signifies a parameter on how much energy from an EMR (electromagnetic radiation) wave a material can absorb;
- Transmission coefficient, which indicates the quantity of EMR penetration through a shield.

Determining the effectiveness of EMI shielding or, more distinctly, determining the attenuation of an EM shield can be very complex as the methods of determining shielding vary with the particularity of application. To figure out the performance of the planer shielding structure, a wide range of standards have been adopted [279]. Generally used techniques for testing shielding strength for plane materials incorporate open-field, coaxial transmission lines, and shielded room tests [280,281].

#### 4.2.1. Open-Field Test Method

The Open-Field Test method, also known as the free-space method, is more suitable for flexible, thin textile substrates. This method is used on a finished product or a finished electronic assembly. The test set-up involves mounting a device at 30 m from a receiving antenna and recording radiated wave emissions. The test requires a spacious open field (approximately 900 m$^2$ area) and no metal or conductive object should be present between the sample and antenna [282].

The measurement procedure of this method contains [282]:

1. Calibration measurement of the transmitted signal without material (P0);
2. Measurements of the transmitted signal as a function of incident angle with material (P1);
3. The ratio of P1/P0 is the power transmittance required to determine complex permittivity.

#### 4.2.2. Shielded Box Method

This method is widely implemented for comparative studies of different shield materials [278]. The test involves a metal box with a port to set samples. A transmitting antenna is placed outside a box, and the receiving antenna is set inside the box. The transmitter sends the signal, and the receiver receives the signal through an open port or a sample fitted over the port. The standard for shielded box methods frequently mentioned is MIL-STD-285-1956—for the frequency range between 100 kHz to 10 GHz [283]. The measurement ranges in this method are given below [284]:

- Low range—9 kHz to 20 MHz—applicable for magnetic components (H);
- Resonant range—20 MHz to 300 MHz—applicable for electrical components (E);
- High range—300 MHz-18 GHz (100 GHz)—in case of plane wave power (P).

The main limitation of this method is the difficulty of achieving proper electrical contact between the shielded box and the specimen [278].

### 4.2.3. Shielded Room Method

The shielded room method is the most delicate, and it was developed to overcome the limitations of the shielded box method. The working principle of this method is the same as the shielded box method, but each component is isolated from the others in separate shielded rooms. An anechoic chamber is used to isolate two antennas; moreover, the specimen size is marginally enlarged by up to 2.5 sqm.

### 4.2.4. Coaxial Transmission Line Method (Transverse Electromagnetic Cell Method)

This method is the most popular and widely used as it is more suitable for measuring small-sized and thin conductive textile samples and extended frequency ranges [285]. One of the main advantages of this method is that the results produced in different labs are comparable. The ASTM D4935 test method is the most preferred method for measuring EMSE of textile materials (planar materials) because of a frequency range of 30 MHz to 1.5 GHz operating in a far-field EM wave as well as a plain wave [278]. The measurements can be executed at a particular frequency range using a modulated signal generator, crystal detector, and tweaked amplifier [281]. The set-up usually consists of coaxial adaptors, signal attenuators, and network analyzers [286]. The net shielding effectiveness originated from absorption and reflection is determined for far-field values. Near-field values may also be measured for electric (E) and magnetic (H) sources from far-field values determined prior [282]. This method has a positive side in that it does not require the thickness measurement of the sample.

A dual TEM (transverse electromagnetic wave) cell method is also used, which allows for measuring the electric and magnetic polarizabilities of test specimens simultaneously [278].

## 5. Application of Conductive Textiles

Electrically conductive textiles are used in various fields, such as the medical, sports, soft robotics, security, and military industries, and as wearable displays [287]. Textile-based electrical components include electrodes, sensors, wearable antennas, wearable displays, actuators, and heating devices [288].

### 5.1. As Electronic Textiles (E-Textiles) for Bio-Sensing and Health Care

People have been investigating the medical applications of electricity in clothing, such as corsets and belts, as early as the 1850s [289]. The first wearable computer was imagined in 1955 by Edward Thorp to predict roulette, terminating in a cooperative endeavor at M.I.T. with Claude Shannon in 1960–1961 [290]. E-textiles, in which electronic functions are integrated more closely within the textile, evolved from wearable computing in the early 1990s. A "Wearable Motherboard" (smart shirt) was developed to monitor the vital signs of humans in an unobtrusive manner, which opened up a new border in healthcare and telemedicine [291]. Scientists conducted additional research on wearable textiles to measure blood pressure, blood oxygen saturation, EEG, EOG, periodic leg movement, core body temperature, and skin temperature in the 2000s [292–296]. A spirometry, a simple test used to help diagnose and monitor certain lung conditions by measuring how much air people can breathe out in one forced breath by pinching noses with a clip and holding a mouthpiece in their mouth, is an uncomfortable condition for the users. An e-textile-based wearable spirometer, Spiro Vest, was demonstrated to gain more comfort than estimated lung behavior from torso–girth movements [297]. E-textiles-based stretch sensors were installed as elbow supports to maintain an ideal setting, and a knitted shirt was used to simulate a daily use setting to prevent caregiver injury in health and medical science [298]. Based on built-in graphene-clad conductive textiles, elastic bands, and lithium batteries for power, a fully wearable smart medical garment comfortably worn around the wrists or neck was reported for ECG monitoring [299]. Sleeping disorders are a major health danger issue

in high-paced modern society. A smart bedsheet using a triboelectric nanogenerator (TENG) with pressure sensitivity, large scalability, and washability for real-time and self-powered sleep behavior monitoring was reported [300]. Waterproof fiber-based strain sensors with a high gauge factor and outstanding stability are necessary for smart textiles, wearable devices, and biomedical electronics. To monitor various human motions (e.g., phonation, pulse, finger bending, and walking), this kind of strain sensor was invented and designed through a combination of PU yarn, multi-layer graphene nanosheets (GNSs)/thin gold film (Au)/GNSs, and a PDMS wrapping layer [301]. Recently, a textile magneto-elastic generator (MEG) was invented that could work as a self-powered sensor for continuous respiratory monitoring with heavy perspiration without any encapsulation [302].

Smart fabric sensors (SFS) are produced by modifying a fabric extrinsically or intrinsically for the sensor properties of SFSs. This can be done in various ways, such as the e-textiles fabrication method, via connectors or electrodes or textile circuitry and elements, encapsulation techniques, and coating. SFS sensors can be categorized as pressure and force sensors, fabric strain sensors, optical fabric sensors, fabric sensors for detecting chemicals and gases, and some parameters such as temperature- and humidity-sensitive fabrics [303]. Sensor development, fabric-based ECG signals, skin–electrode interface improvement, sensing shirts, and belts for sleep measurement were investigated. Different parameters, including movement, posture, and temperature, were reviewed and compared to the innovations in the textile field [304]. Figure 8 shows the construction of an ECG detecting smart garment as an example. The ECG sensor patches (5) were placed inside the undershirt ("1. 2." outside and inside faces for men or the bra strap "3. 4." for women). (6) Cross-sectional view of the textile electrode (hitoe®). The cloth of polyester nanofiber (8) was coated by electroconductive polymer PEDOT-PSS (7, blue circles), and its surface was directly placed on the skin (9). The back side of the electroconductive textile was fixed on the waterproof layer (12) and the cloth of the underwear (12). ECG signals were conducted through the textile electrodes (5. 10. 11) to electroconductive yarn (15) and a snap hook button (14); then, these ECG electrodes and the lead wire were connected to the ECG transmitter (13).



**Figure 8.** Components of an ECG detecting smart garment. Reprinted from [305].

The electrodes in e-textiles were used specifically to determine biomedical features such as oxygen, moisture, contaminants, or salinity. Different fabrication techniques can be used [306]. The application of smart textiles in the physiological field, such as blood glucose level, blood pressure, respiration rate, body temperature, physical activity monitoring, and rehabilitation, was discussed [307]. Electronic, pneumatic, and electropneumatic transducers were studied to measure the interface pressure. The avoidance of sickness can be attained with this type of soft sensor. The use of wrist wearable instruments and a central monitoring system were mentioned to enhance the speed of assessing a patient's condition. The use of ambulatory devices was investigated for mobility and improved healthcare [308].

Humans stretch their bodies to their limits during sports activities or leisure-type amateur training. To get a better result and stretch the personal limit results in muscular and thermophysiological stresses, the garment does not add any further stress; it should, if possible, help the athletes sit, get a better result, and prevent sports injuries [309]. A device named "The Intelligent Knee Sleeve" (IKS) (see Figure 9) was used in football and other sports training to avoid disabling injuries during movements involving rapid deceleration, quick changes of direction, and sudden landings. The IKS consists of a simple, elastic sleeve incorporating disposable PPy-coated nylon-lycra fabric, integrated with appropriate electronic circuitry (3 V) sensor placed over the kneecap, and provides feedback as audio to alert the desired flexion limit [310]. During exercise, a major problem is water loss, including hypersensitivity, headache, dizziness, convulsions, vomiting, increased body temperature and heart rate, increased perceived power, decreased mental function, and delayed gastric emptying [311].



**Figure 9.** The intelligent knee sleeve [310] (reprinted with permission from Elsevier).

A device was invented to detect increased pH levels using polyamide/lycra blended fabric and a pH sensor for sweat collection and real-time pH monitoring up to 0.2 pH units in 2008 [312]. To prevent knee injury and determine the user's bending angle and tensile deformation, the PU/PEDOT:PSS-based knitted textile sensor integrated with a wireless transmitter that was used as a knee sleeve was demonstrated [313]. A pre-treatment process of the surface of organic nanoparticle-based inkjet printable textile was reported, which enabled all inkjet-printed graphene-based wearable e-textiles to be breathable, comfortable, and environmentally friendly, and measured the CG signal [262]. Using multiscale disordered porous polyurethane (MPPU) via microfluid spinning, self-sensing and self-cooling properties were invented. It could reduce the temperature by around 2.5 degrees Celsius between skin and apparel compared to cotton [314].

### 5.2. Soft Robotics

Soft robotics is a branch of robotics that involves constructing robot bodies and actuators using extremely soft or expansible materials [315]. Future soft actuation technologies could utilize conductive textiles as electrode materials of sensing transducers that can be resistive or piezoresistive with a wide variety of sensing functionality, including shape reconstruction, bending angle, direction, contraction length, or circumference [316]. Conductive yarns demonstrate electric actuation by changing the distance of twisted fibers by electromagnetic or electrostatic force [317]. A PVC gel-based actuator comprised of a PVC inner core and insulated PVC shell was designed. A pair of identical fibers that were loosely twisted together got closer together and resulted in the elongation of yarn when voltage was applied to the two fibers' inner cores. A textile-type and a yarn-type actuator were constructed, and a maximum contraction strain of 53% and an expansion ratio of 1.4% were achieved, respectively [318]. A planer DE (Dielectric Elastomer) actuator, bending DE actuator, and EA (electro-adhesive) actuator have been developed and tested. Under 9 kV and 6 kV, relative expansion rates of 16.4% and 5% were achieved for the planer and bending DE actuators, respectively. Additionally, under 5 kV, the shear adhesive of 0.14 kPa was obtained for the EA actuator. Furthermore, a crawling robot driven by the above actuators has been developed, traveling 18 mm distance in 3 min [319]. An octopus-inspired continuum robot arm was constructed based on a conductive textile material called Electrolycra (Mindsets Ltd., Saffron Walden, UK) [320]. A bending sensor was developed for a robotic glove in which a dielectric silicone was employed as the sensing material, which was placed between conductive knitted electrodes manufactured from silver-coated yarn.

Additionally, the sensor mat was set parallel to the Wales structure, which was sounded with extra silicone [321]. Atalay et al. designed a new shape-sensing system based on electroconductive yarn material integrated into a soft manipulator with pneumatic actuation, which is suitable for implementation in miniature surgical instruments [321]. Mehmet et al. built an artificial muscle with actuating and sensing functions [322]. The bimorph tendril-like fiber was created by thermally pulling cyclic olefin co-polymer elastomer and polyethylene. As a resistance strain sensor, a coating of conductive nanowire mesh was applied to the fiber. The fiber contracted as it was heated, and the electrode's resistance monitored the contraction and elongation based on piezoresistive feedback.

Furthermore, a humanoid limb was fitted with sensor-fitted fiber actuators. When heated with a hot gun, the fiber actuators contracted, causing the artificial limb to bend, and the resistance change of the electrodes was used to determine the bending angle of the limb [317]. A highly stretchable and durable conductive knitted fabric was developed and applied to the covering of a paper–fabric composite-based actuator, which has the potential as the electronic skin of soft robots. The electrical resistance of the fabric was sustained under a maximum average membrane strain of 300% in 3D deformation. The fabric was capable of withstanding more than 1,200,000 cycles of loading under 20% tensile strain and 10,000 abrasion cycles [323].

### 5.3. Other E-textiles Applications

The demand for electronic yarn or e-yarn is increasing day by day. A prototype to produce e-yarn—as can be seen in Figure 10—using the encapsulation process was reported to be incorporated into the fabric via knitting and weaving machinery that can meet the demand for electronic textile material [324].
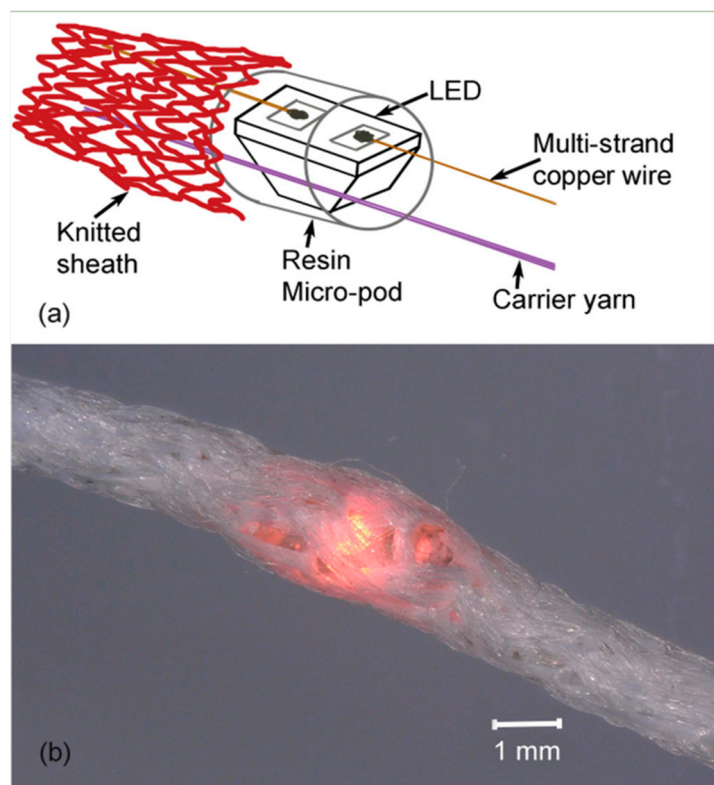
**Figure 10.** (**a**) A schematic diagram showing the e-yarn (electronic yarn) structure, with an LED (light-emitting diode) protected by a micro pod and surrounded by a knitted sheath. (**b**) A completed e-yarn containing an LED (illuminated) shown at 30× magnification (reprinted from [324]).

Due to their softness, breathability, and biocompatibility, wearable e-textiles have attracted increasing appeal, making them long-lasting and wearable in the long run. A multifunctional integration system with thermal insulation, Joule heating, and particulate matter (PM) filter features was reported using conductive nanowires [325]. Several companies, including Google, which is developing capacitive touching textiles in its Google Jacquard project, have recognized the potential of electronic wearable textiles. This project enables a seamless and dependable wearable computing concept that can assist customers in performing daily tasks, such as answering phone calls without interrupting an ongoing activity [326].

### 5.4. EM Shielding Textiles

The rapid expansion of electronic technologies and the vast spread of advanced electrical components in automation, communications, space, computations, and other sectors have introduced the adverse effects of electromagnetic interference (EMI)—mainly in the radio frequency ranging from $10^4$ to $10^{12}$ Hz. Many international radiation regulatory bodies, such as the Australian Radiation Protection and Nuclear Safety Agency Standard (ARPANSA) and International Commission on Non-ionizing Radiation Protection (ICNIRP), have set the safety limit for a specific absorption rate of radiation within 2 WKg$^{-1}$ of human tissue [327,328]. Wearable EM shielding has become a crucial demand to prevent adverse biological effects, such as raising human eye temperature [329], damaging the human

tissues, leading to childhood cancer [330], and even causing hazardous effects on the human reproduction system [331] from EM radiation generated from electrical devices.

A distinguished aspect of conductive textiles is that they can interact with electromagnetic radiation (EMR) by absorbing and deflecting EM waves [278]. This feature facilitates the employment of conductive textiles in EM shielding devices very solemnly. CNT/PANI-coated fabrics were developed, which exhibited a low sheet resistance ($20.1 \pm 1.7$ $\Omega$/sq) along with a moderate range of EMI SE of 23 dB over the frequency range of 4–6 GHz (C-band) and possessed high EMSE retention against various treatments such as wash, sonication, acidic, and alkali [332]. Zhu et al. reported eco-friendly EM shielding textiles consisting of SWCNT, biomass-derived chitosan, and glucaric acid coatings, which retained a convenient EMI SE of 30 dB and better durability than Ag or Ag/polymer composite-film-coated textiles [333]. Yin et al. described multi-layered PANI/MXene/CF fabrics with appropriate EMI shielding properties (26 dB) included with high specific shielding effectiveness (135.5 dB·cm$^3$/g) [334]. In another study, they coated 1D PANI NW/2D MXene nanosheets/carbon fiber fabrics with PDS, resulting in an outstanding increase in EMI shielding performance (SE = 35.3 dB, SSE = 63.8 dB·cm$^3$/g) even at a very low thickness (0.376 mm) with a convenient self-cleaning and air permeability performance, which would provide great access to commercial EMI shielding textiles [335]. Jia et al. demonstrated a machine washable, highly conductive (1227 Sm$^{-1}$) EMI shielding textile prepared with PU/AgNWs, which exhibited an excellent SE of 63.9 dB—even at a lower density (0.34 gcm$^{-3}$) and thickness (0.6 mm) compared to other metallic shielding textiles based on AgNW, copper nanowire (CuNW), and CNTs—and it could be integrated even in harsh conditions with long-term EMI shielding durability [336]. Wang et al. reported a water-resistant, breathable, mechanically robust PDMS-coated nickel ferrite/MWCNTs/cotton fabrics with a superior EM SE of 84.5 dB in the X-band and an outstanding EMI SE retention (above 90%) against washing cycles [169]. AgNW/Fe$_3$O$_4$/PDMS coating was integrated on cotton fabrics, having an outstanding EMI SE of 100.9 dB, which could withstand extreme acidic (pH = 2) and alkali (pH = 12) conditions and retain about 96% and 99% of SE retention, respectively [337]. An ultrahigh SE of 106 dB was evaluated for AgNW/PU/carbon fiber fabrics that retained 95.8 dB of SE even after 100 peeling cycles [338].

Shielding effectiveness (SE) is the total shielding through absorption (SE$_a$), reflection (SE$_r$), and multiple reflections (SE$_m$). SE due to multiple reflections (SE$_m$) is neglected for practical applications when the SE due to absorption is higher than 10 dB [339].

*5.5. Supercapacitor*

With the rising demand for fast charging as well as high energy storing devices and the growing concern for human comfort in the wearable smart textiles industry, textile-based supercapacitors are making a revolutionary step due to some of their unique features, such as their extreme wearability, flexibility, comfort, durability, effective electrochemical redox performance, and cost-effective production process [340].

The energy storage performance of supercapacitors is mainly dependent on selecting the electrode and electrolyte materials; moreover, the development of supercapacitors concerning flexibility with comfort and a combination of supercapacitors with textile fabric is resulting in a revolution [341–343]. Consequently, a large amount of research has been done to develop advanced electrode materials for flexible supercapacitors with suitable structural properties with deformation, stretching, bending, and washability [344,345].

Song et al. reported textile-based electrodes for supercapacitors composed of PANI/G/HCL through a simple dipping and drying process of graphene on fabrics followed by in situ polymerization of aniline, which exhibited an impressive areal specific capacitance of 1601 mF cm$^{-2}$ at the current density of 1 mA cm$^{-2}$. In contrast, over 75% of initial area-specific capacitance was preserved after 10,000 cycles [346]. The deposition of rGO and SnO$_2$ on textile fabric via supersonic spraying showed the highest specific capacitance of 1008 mF cm$^{-2}$ at a current loading of 1.5 mA cm$^{-2}$, with a capacitance retention of 93% after 10,000 cycles [347].

Lu et al. designed a flexible electrode with a high specific surface area provided by metal–organic frameworks (MOFs) and flexibility provided by CNTs [348]. The performance of that supercapacitor showed a stable energy supply under cyclic deformations and even wearable conditions. Mechanically strengthened ultralong $MnO_2$ nanowire composites were developed as a stretchable electrode that showed a specific capacitance of 227.2 mF cm$^{-2}$ and can be stretched up to 500% without degradation of electrochemical performance. Around 98% of the initial capacitance after 10,000 stretch-and-release cycles was performed under 400% tensile strain [349].

## 6. Challenges and Future Outlook

During the past two decades, conductive textiles have been a promising segment of textile engineering and have drawn significant research interest. Though outstanding progress has been achieved in this segment through the relentless effort of researchers, there are still some challenges that hinder the commercialization of conductive textiles on a large scale. Most of the textile materials are not conductive, and it is a daunting challenge to make them conductive by incorporating conductive materials within them. There are several challenges to conductive textiles, including connectivity, textiles and conductive materials and their fabrication, and wear of the materials [350]. Besides these challenges, the designer faces some challenges during the prosperity of conductive textiles, such as mechanical environment, washability of the textiles, power supplies in the circuit, commercialization, and cost of the conductive materials [5]. Durability is one of the major concerns for conductive textiles because textiles are prone to wear abrasion, bending of the coated materials, and stretching [351]. The mechanical characteristics of textiles sensors resist being flexible and permeable to air and water [249]. The mass production of conductive textiles is challenging due to the self-energy generation form and the high number of elements [288]. The textile sensor is one of the widespread areas of conductive textiles in which the conventional concept of attaching the solid-state electrical components with textile materials has been turned into flexible e-textiles capable of sensing various phenomena. Until now, one of the major challenges in this regard is maintaining the efficiency of these textile sensors compared to the solid components [352]. The challenge with textile connectors is maintaining the connectivity eminently through the complete textile surface during the assembling stage of developing wearable e-textiles [353]. The textile composite electrode has drawn eminent attention to converting conventional batteries and supercapacitors into flexible energy storage devices. Some challenges are still present to pave the way for the commercialized production of these flexible electrodes. These possess relatively higher resistance, reduced mechanical strength of yarn-like electrodes, and lower energy density than rigid-state batteries and supercapacitors [354]. Higher resistance is mainly due to textiles' porous structures and lower intrinsic conductive nature. Textile yarn-like electrodes seem more vulnerable to mechanical stress, resulting in more yarn breakage during the fabrication process than conventional yarn [355]. This indicates a challenge to maintaining the high speed of industrial machinery during the fabrication process of these electrodes. Future researchers should focus on these challenges of conductive textiles to pave the way for large-scale commercial production of these materials.

## 7. Conclusions

This review has highlighted various fabrication methods for conductive textiles with detailed information about conductive polymers. Research should be carried out to eliminate the disadvantages of various coating and printing methods of imparting conductivity. Graphene has become the center of fascination for researchers for its extraordinary properties. Smart textiles with electrical conductivity and signal-sensing capabilities are gaining more and more attention due to their various applications. E-textiles face many challenges, such as washability, power supply, product development, and commercialization, from users' perspective. There is a huge research gap in this aspect to investigate post-usage problems and the development of solutions.

## References

1. Mattila, H. Chapter 15—Yarn to Fabric: Intelligent Textiles. In *Textiles and Fashion*; Sinclair, R., Ed.; Woodhead Publishing: Cambridge, UK, 2015; pp. 355–376. [CrossRef]
2. Guler, S.D.; Gannon, M.; Sicchio, K. (Eds.) A Brief History of Wearables. In *Crafting Wearables: Blending Technology with Fashion*; Apress: Berkeley, CA, USA, 2016; pp. 3–10. [CrossRef]
3. Tseghai, G.B.; Mengistie, D.A.; Malengier, B.; Fante, K.A.; Van Langenhove, L. PEDOT:PSS-Based Conductive Textiles and Their Applications. *Sensors* **2020**, *20*, 1881. [CrossRef] [PubMed]
4. Köhler, A.R. Challenges for eco-design of emerging technologies: The case of electronic textiles. *Mater. Des.* **2013**, *51*, 51–60. [CrossRef]
5. Cherenack, K.; van Pieterson, L. Smart textiles: Challenges and opportunities. *J. Appl. Phys.* **2012**, *112*, 091301. [CrossRef]
6. Hughes-Riley, T.; Dias, T.; Cork, C. A Historical Review of the Development of Electronic Textiles. *Fibers* **2018**, *6*, 34. [CrossRef]
7. Elschner, A.; Kirchmeyer, S.; Lovenich, W.; Merker, U.; Reuter, K. *PEDOT: Principles and Applications of an Intrinsically Conductive Polymer*, 1st ed.; CRC Press: Boca Raton, FL, USA, 2010. [CrossRef]
8. Varnaitė-Žuravliova, S. *The Types, Properties, and Applications of Conductive Textiles*; Cambridge Scholars Publishing: Newcastle Upon Tyne, UK, 2019.
9. Grancarić, A.M.; Jerkovic, I.; Koncar, V.; Cochrane, C.; Kelly, F.M.; Soulat, D.; Legrand, X. Conductive polymers for smart textile applications. *J. Ind. Text.* **2017**, *48*, 612–642. [CrossRef]
10. Deshmukh, K.; Basheer Ahamed, M.; Deshmukh, R.R.; Khadheer Pasha, S.K.; Bhagat, P.R.; Chidambaram, K. 3-Biopolymer composites with high dielectric performance: Interface engineering. In *Biopolymer Composites in Electronics*; Sadasivuni, K.K., Ponnamma, D., Kim, J., Cabibihan, J.-J., AlMaadeed, M.A., Eds.; Elsevier: Amsterdam, The Netherlands, 2017; pp. 27–128. [CrossRef]
11. Tatari, A.; Shekarian, E.; Ghaffari, M.; Akbarpour, I. Production and applications of paper-conductive polymer composites. *J. Prot. Exploit. Nat. Resour.* **2017**, *6*, 27–37. [CrossRef]
12. Sun, K.; Zhang, S.; Li, P.; Xia, Y.; Zhang, X.; Du, D.; Isikgor, F.H.; Ouyang, J. Review on application of PEDOTs and PEDOT:PSS in energy conversion and storage devices. *J. Mater. Sci. Mater. Electron.* **2015**, *26*, 4438–4462. [CrossRef]
13. Yussuf, A.; Al-Saleh, M.; Al-Enezi, S.; Abraham, G. Synthesis and Characterization of Conductive Polypyrrole: The Influence of the Oxidants and Monomer on the Electrical, Thermal, and Morphological Properties. *Int. J. Polym. Sci.* **2018**, *2018*, 1–8. [CrossRef]
14. Machida, S.; Miyata, S.; Techagumpuch, A. Chemical synthesis of highly electrically conductive polypyrrole. *Synth. Met.* **1989**, *31*, 311–318. [CrossRef]
15. Noh, K.A.; Kim, D.-W.; Jin, C.-S.; Shin, K.-H.; Kim, J.H.; Ko, J.M. Synthesis and pseudo-capacitance of chemically-prepared polypyrrole powder. *J. Power Sources* **2003**, *124*, 593–595. [CrossRef]
16. Stankovic, R.; Laninović, V.; Vojnović, M.; Pavlović, O.; Krstajić, N.; Jovanovic, S. Synthesis and Electrochemical Properties of Polypyrrole. *Mater. Sci. Forum* **1996**, *214*, 147–154. [CrossRef]
17. Park, J.H.; Ko, J.M.; Park, O.; Kim, D.-W. Capacitance properties of graphite/polypyrrole composite electrode prepared by chemical polymerization of pyrrole on graphite fiber. *J. Power Sources* **2002**, *105*, 20–25. [CrossRef]
18. An, K.H.; Jeon, K.K.; Heo, J.K.; Lim, S.C.; Bae, D.J.; Lee, Y.H. High-Capacitance Supercapacitor Using a Nanocomposite Electrode of Single-Walled Carbon Nanotube and Polypyrrole. *J. Electrochem. Soc.* **2002**, *149*, A1058–A1062. [CrossRef]
19. An, K.H.; Jeong, S.Y.; Hwang, H.R.; Lee, Y.H. Enhanced Sensitivity of a Gas Sensor Incorporating Single-Walled Carbon Nanotube–Polypyrrole Nanocomposites. *Adv. Mater.* **2004**, *16*, 1005–1009. [CrossRef]
20. Sahoo, N.G.; Jung, Y.C.; So, H.H.; Cho, J.W. Polypyrrole coated carbon nanotubes: Synthesis, characterization, and enhanced electrical properties. *Synth. Met.* **2007**, *157*, 374–379. [CrossRef]
21. Humpolicek, P.; Kasparkova, V.; Saha, P.; Stejskal, J. Biocompatibility of polyaniline. *Synth. Met.* **2012**, *162*, 722–727. [CrossRef]
22. Li, Q.; Wu, J.; Tang, Q.; Lan, Z.; Li, P.; Lin, J.; Fan, L. Application of microporous polyaniline counter electrode for dye-sensitized solar cells. *Electrochem. Commun.* **2008**, *10*, 1299–1302. [CrossRef]
23. Kulkarni, V.G.; Campbell, L.D.; Mathew, W.R. Thermal stability of polyaniline. *Synth. Met.* **1989**, *30*, 321–325. [CrossRef]
24. Mengoli, G.; Musiani, M.M.; Zotti, G.; Valcher, S. Potentiometric investigation of the kinetics of the polyaniline—Oxygen reaction. *J. Electroanal. Chem. Interfacial Electrochem.* **1986**, *202*, 217–230. [CrossRef]
25. Stejskal, J.; Kratochvíl, P.; Jenkins, A.D. Polyaniline: Forms and Formation. *Collect. Czechoslov. Chem. Commun.* **1995**, *60*, 1747–1755. [CrossRef]

26. Zarrintaj, P.; Vahabi, H.; Saeb, M.R.; Mozafari, M. Chapter 14—Application of polyaniline and its derivatives. In *Fundamentals and Emerging Applications of Polyaniline*; Elsevier: Amsterdam, The Netherlands, 2019; pp. 259–272. [CrossRef]

27. Bhadra, S.; Khastgir, D.; Singha, N.K.; Lee, J.H. Progress in preparation, processing and applications of polyaniline. *Prog. Polym. Sci.* **2009**, *34*, 783–810. [CrossRef]

28. Beygisangchin, M.; Abdul Rashid, S.; Shafie, S.; Sadrolhosseini, A.; Lim, H. Preparations, Properties, and Applications of Polyaniline and Polyaniline Thin Films—A Review. *Polymers* **2021**, *13*, 2003. [CrossRef] [PubMed]

29. Tang, X.; Tian, M.; Qu, L.; Zhu, S.; Guo, X.; Han, G.; Sun, K.; Hu, X.; Wang, Y.; Xu, X. Functionalization of cotton fabric with graphene oxide nanosheet and polyaniline for conductive and UV blocking properties. *Synth. Met.* **2015**, *202*, 82–88. [CrossRef]

30. Wu, W.; Wang, B.; Segev-Bar, M.; Dou, W.; Niu, F.; Horev, Y.D.; Deng, Y.; Plotkin, M.; Huynh, T.-P.; Jeries, R.; et al. Free-Standing and Eco-Friendly Polyaniline Thin Films for Multifunctional Sensing of Physical and Chemical Stimuli. *Adv. Funct. Mater.* **2017**, *27*, 1703147. [CrossRef]

31. McCullough, R.D. The Chemistry of Conducting Polythiophenes: From Synthesis to Self-Assembly to Intelligent Materials. In *Handbook of Oligo- and Polythiophenes*; John Wiley & Sons: New York, NY, USA, 1998; pp. 1–44. [CrossRef]

32. Sotzing, G.A.; Reynolds, J.R.; Steel, P.J. Poly(3,4-ethylenedioxythiophene) (PEDOT) prepared via electrochemical polymerization of EDOT, 2,2′-Bis(3,4-ethylenedioxythiophene) (BiEDOT), and their TMS derivatives. *Adv. Mater.* **1997**, *9*, 795–798. [CrossRef]

33. Fabretto, M.; Jariego-Moncunill, C.; Autere, J.-P.; Michelmore, A.; Short, R.; Murphy, P. High conductivity PEDOT resulting from glycol/oxidant complex and glycol/polymer intercalation during vacuum vapour phase polymerisation. *Polymer* **2011**, *52*, 1725–1730. [CrossRef]

34. Kirchmeyer, S.; Reuter, K. Scientific importance, properties and growing applications of poly(3,4-ethylenedioxythiophene). *J. Mater. Chem.* **2005**, *15*, 2077–2088. [CrossRef]

35. O'Connor, T.F.; Zaretski, A.V.; Savagatrup, S.; Printz, A.D.; Wilkes, C.D.; Diaz, M.I.; Sawyer, E.J.; Lipomi, D.J. Wearable organic solar cells with high cyclic bending stability: Materials selection criteria. *Sol. Energy Mater. Sol. Cells* **2016**, *144*, 438–444. [CrossRef]

36. Li, Z.; Ma, G.; Ge, R.; Qin, F.; Dong, X.; Meng, W.; Liu, T.; Tong, J.; Jiang, F.; Zhou, Y.; et al. Free-Standing Conducting Polymer Films for High-Performance Energy Devices. *Angew. Chem. Int. Ed.* **2015**, *55*, 979–982. [CrossRef]

37. Ding, Y.; Invernale, M.A.; Sotzing, G.A. Conductivity Trends of PEDOT-PSS Impregnated Fabric and the Effect of Conductivity on Electrochromic Textile. *ACS Appl. Mater. Interfaces* **2010**, *2*, 1588–1593. [CrossRef]

38. Hamedi, M.; Herland, A.; Karlsson, R.H.; Inganäs, O. Electrochemical Devices Made from Conducting Nanowire Networks Self-Assembled from Amyloid Fibrils and Alkoxysulfonate PEDOT. *Nano Lett.* **2008**, *8*, 1736–1740. [CrossRef] [PubMed]

39. Wang, G.-F.; Tao, X.-M.; Wang, R.-X. Fabrication and characterization of OLEDs using PEDOT:PSS and MWCNT nanocomposites. *Compos. Sci. Technol.* **2008**, *68*, 2837–2841. [CrossRef]

40. Li, Z.; Sinha, S.K.; Treich, G.M.; Wang, Y.; Yang, Q.; Deshmukh, A.A.; Sotzing, G.A.; Cao, Y. All-organic flexible fabric antenna for wearable electronics. *J. Mater. Chem. C* **2020**, *8*, 5662–5667. [CrossRef]

41. Liu, L.; Yu, Y.; Yan, C.; Li, K.; Zheng, Z. Wearable energy-dense and power-dense supercapacitor yarns enabled by scalable graphene–metallic textile composite electrodes. *Nat. Commun.* **2015**, *6*, 7260. [CrossRef] [PubMed]

42. Miura, H.; Fukuyama, Y.; Sunda, T.; Lin, B.; Zhou, J.; Takizawa, J.; Ohmori, A.; Kimura, M. Foldable Textile Electronic Devices Using All-Organic Conductive Fibers. *Adv. Eng. Mater.* **2014**, *16*, 550–555. [CrossRef]

43. Liu, N.; Fang, G.; Wan, J.; Zhou, H.; Long, H.; Zhao, X. Electrospun PEDOT:PSS–PVA nanofiber based ultrahigh-strain sensors with controllable electrical conductivity. *J. Mater. Chem.* **2011**, *21*, 18962–18966. [CrossRef]

44. Lock, J.P.; Im, S.G.; Gleason, K.K. Oxidative Chemical Vapor Deposition of Electrically Conducting Poly(3,4-ethylenedioxythiophene) Films. *Macromolecules* **2006**, *39*, 5326–5329. [CrossRef]

45. Brooke, R.; Mitraka, E.; Sardar, S.; Sandberg, M.; Sawatdee, A.; Berggren, M.; Crispin, X.; Jonsson, M.P. Infrared electrochromic conducting polymer devices. *J. Mater. Chem. C* **2017**, *5*, 5824–5830. [CrossRef]

46. Fabretto, M.; Autere, J.-P.; Hoglinger, D.; Field, S.; Murphy, P. Vacuum vapour phase polymerised poly(3,4-ethyelendioxythiophene) thin films for use in large-scale electrochromic devices. *Thin Solid Films* **2011**, *519*, 2544–2549. [CrossRef]

47. Kaushik, V.; Lee, J.; Hong, J.; Lee, S.; Lee, S.; Seo, J.; Mahata, C.; Lee, T. Textile-Based Electronic Components for Energy Applications: Principles, Problems, and Perspective. *Nanomaterials* **2015**, *5*, 1493–1531. [CrossRef]

48. Meng, Q.; Cai, K.; Du, Y.; Chen, L. Preparation and thermoelectric properties of SWCNT/PEDOT:PSS coated tellurium nanorod composite films. *J. Alloy. Compd.* **2018**, *778*, 163–169. [CrossRef]

49. Chen, M.; Duan, S.; Zhang, L.; Wang, Z.; Li, C. Three-dimensional porous stretchable and conductive polymer composites based on graphene networks grown by chemical vapour deposition and PEDOT:PSS coating. *Chem. Commun.* **2014**, *51*, 3169–3172. [CrossRef] [PubMed]

50. Zimmermann, Y.; Neudeck, A.; Möhring, U. Metal-coated fibers. In *Inorganic and Composite Fibers: Production, Properties, and Applications*; Elsevier: Cambridge, UK, 2018; pp. 243–276. [CrossRef]

51. Montazer, M.; Harifi, T. *Nanofinishing of Textile Materials*, 1st ed.; Woodhead Publishing: Cambridge, UK, 2018.

52. Atwa, Y.; Maheshwari, N.; Goldthorpe, I.A. Silver nanowire coated threads for electrically conductive textiles. *J. Mater. Chem. C* **2015**, *3*, 3908–3912. [CrossRef]

53. Silva, I.O.; Ladchumananandasivam, R.; Nascimento, J.H.O.; Silva, K.K.O.S.; Oliveira, F.R.; Souto, A.P.; Felgueiras, H.P.; Zille, A. Multifunctional Chitosan/Gold Nanoparticles Coatings for Biomedical Textiles. *Nanomaterials* **2019**, *9*, 1064. [CrossRef]

54. Wu, Y.; Mechael, S.S.; Chen, Y.; Carmichael, T.B. Solution Deposition of Conformal Gold Coatings on Knitted Fabric for E-Textiles and Electroluminescent Clothing. *Adv. Mater. Technol.* **2018**, *3*, 1700292. [CrossRef]

55. Wang, X.; Yan, C.; Hu, H.; Zhou, X.; Guo, R.; Liu, X.; Xie, Z.; Huang, Z.; Zheng, Z. Aqueous and Air-Compatible Fabrication of High-Performance Conductive Textiles. *Chem.-Asian J.* **2014**, *9*, 2170–2177. [CrossRef]

56. Irene, G.; Georgios, P.; Ioannis, C.; Anastasios, T.; Diamantis, P.; Marianthi, C.; Philippe, W.; Maria, S. Copper-coated textiles: Armor against MDR nosocomial pathogens. *Diagn. Microbiol. Infect. Dis.* **2016**, *85*, 205–209. [CrossRef]

57. Ali, A.; Baheti, V.; Militky, J.; Khan, Z.; Tunakova, V.; Naeem, S. Copper coated multifunctional cotton fabrics. *J. Ind. Text.* **2017**, *48*, 448–464. [CrossRef]

58. Gouda, M.; Aljaafari, A.; Al-Fayz, Y.; Boraie, W.E. Preparation and Characterization of Some Nanometal Oxides Using Microwave Technique and Their Application to Cotton Fabrics. *J. Nanomater.* **2015**, *2015*, 1–9. [CrossRef]

59. Zeng, W.; Shu, L.; Li, Q.; Chen, S.; Wang, F.; Tao, X.M. Fiber-Based Wearable Electronics: A Review of Materials, Fabrication, Devices, and Applications. *Adv. Mater.* **2014**, *26*, 5310–5336. [CrossRef]

60. Yapici, M.K.; Alkhidir, T.; Samad, Y.A.; Liao, K. Graphene-clad textile electrodes for electrocardiogram monitoring. *Sens. Actuators B Chem.* **2015**, *221*, 1469–1474. [CrossRef]

61. Li, L.; Fan, T.; Hu, R.; Liu, Y.; Lu, M. Surface micro-dissolution process for embedding carbon nanotubes on cotton fabric as a conductive textile. *Cellulose* **2016**, *24*, 1121–1128. [CrossRef]

62. Sankaran, S.; Deshmukh, K.; Ahamed, M.B.; Pasha, S.K. Recent advances in electromagnetic interference shielding properties of metal and carbon filler reinforced flexible polymer composites: A review. *Compos. Part A Appl. Sci. Manuf.* **2018**, *114*, 49–71. [CrossRef]

63. Thostenson, E.T.; Ren, Z.; Chou, T.-W. Advances in the science and technology of carbon nanotubes and their composites: A review. *Compos. Sci. Technol.* **2001**, *61*, 1899–1912. [CrossRef]

64. Huang, X.; Yin, Z.; Wu, S.; Qi, X.; He, Q.; Zhang, Q.; Yan, Q.; Boey, F.; Zhang, H. Graphene-Based Materials: Synthesis, Characterization, Properties, and Applications. *Small* **2011**, *7*, 1876–1902. [CrossRef]

65. Choudhary, N.; Hwang, S.; Choi, W. *Carbon Nanomaterials: A Review in Handbook of Nanomaterials Properties*; Springer: Berlin, Germany, 2014; pp. 709–769. [CrossRef]

66. Iijima, S. Helical microtubules of graphitic carbon. *Nature* **1991**, *354*, 56–58. [CrossRef]

67. Iijima, S.; Ichihashi, T. Single-shell carbon nanotubes of 1-nm diameter. *Nature* **1993**, *363*, 603–605. [CrossRef]

68. Dai, H.; Rinzler, A.G.; Nikolaev, P.; Thess, A.; Colbert, D.T.; Smalley, R.E. Single-wall nanotubes produced by metal-catalyzed disproportionation of carbon monoxide. *Chem. Phys. Lett.* **1996**, *260*, 471–475. [CrossRef]

69. Yu, M.-F.; Lourie, O.; Dyer, M.J.; Moloni, K.; Kelly, T.F.; Ruoff, R.S. Strength and Breaking Mechanism of Multiwalled Carbon Nanotubes Under Tensile Load. *Science* **2000**, *287*, 637–640. [CrossRef]

70. Yu, M.-F.; Files, B.S.; Arepalli, S.; Ruoff, R.S. Tensile Loading of Ropes of Single Wall Carbon Nanotubes and their Mechanical Properties. *Phys. Rev. Lett.* **2000**, *84*, 5552–5555. [CrossRef]

71. Cao, Q.; Yu, Q.; Connell, D.W.; Yu, G. Titania/carbon nanotube composite ($TiO_2$/CNT) and its application for removal of organic pollutants. *Clean Technol. Environ. Policy* **2013**, *15*, 871–880. [CrossRef]

72. Wei, B.Q.; Vajtai, R.; Ajayan, P.M. Reliability and current carrying capacity of carbon nanotubes. *Appl. Phys. Lett.* **2001**, *79*, 1172–1174. [CrossRef]

73. Dürkop, T.; Kim, B.M.; Fuhrer, M.S. Properties and applications of high-mobility semiconducting nanotubes. *J. Phys. Condens. Matter* **2004**, *16*, R553–R580. [CrossRef]

74. Terrones, M. Science and technology of the twenty first century: Synthesis, properties, and applications of carbon nanotubes. *Ann. Rev. Mater. Res.* **2003**, *33*, 419–501. [CrossRef]

75. Dillon, A.C.; Jones, K.M.; Bekkedahl, T.A.; Kiang, C.H.; Bethune, D.S.; Heben, M.J. Storage of hydrogen in single-walled carbon nanotubes. *Nature* **1997**, *386*, 377–379. [CrossRef]

76. Gao, B.; Bower, C.; Lorentzen, J.; Fleming, L.; Kleinhammes, A.; Tang, X.; McNeil, L.; Wu, Y.; Zhou, O. Enhanced saturation lithium composition in ball-milled single-walled carbon nanotubes. *Chem. Phys. Lett.* **2000**, *327*, 69–75. [CrossRef]

77. Raffaelle, R.; Landi, B.; Harris, J.; Bailey, S.; Hepp, A. Carbon nanotubes for power applications. *Mater. Sci. Eng. B* **2005**, *116*, 233–243. [CrossRef]

78. Vairavapandian, D.; Vichchulada, P.; Lay, M.D. Preparation and modification of carbon nanotubes: Review of recent advances and applications in catalysis and sensing. *Anal. Chim. Acta* **2008**, *626*, 119–129. [CrossRef]

79. Artukovic, E.; Kaempgen, M.; Hecht, D.S.; Roth, A.S.; Grüner, G. Transparent and Flexible Carbon Nanotube Transistors. *Nano Lett.* **2005**, *5*, 757–760. [CrossRef]

80. Lee, J.U.; Gipp, P.P.; Heller, C.M. Carbon nanotube p-n junction diodes. *Appl. Phys. Lett.* **2004**, *85*, 145–147. [CrossRef]

81. Li, J.; Hu, L.; Wang, L.; Zhou, Y.; Grüner, G.; Marks, T.J. Organic Light-Emitting Diodes Having Carbon Nanotube Anodes. *Nano Lett.* **2006**, *6*, 2472–2477. [CrossRef] [PubMed]

82. Li, Z.; Dharap, P.; Nagarajaiah, S.; Barrera, E.V.; Kim, J.D. Carbon Nanotube Film Sensors. *Adv. Mater.* **2004**, *16*, 640–643. [CrossRef]

83. Mahar, B.; Laslau, C.; Yip, R.; Sun, Y. Development of Carbon Nanotube-Based Sensors—A Review. *IEEE Sens. J.* **2007**, *7*, 266–284. [CrossRef]

84. Novoselov, K.S.; Geim, A.K.; Morozov, S.V.; Jiang, D.; Katsnelson, M.I.; Grigorieva, I.V.; Dubonos, S.V.; Firsov, A.A. Two-dimensional gas of massless Dirac fermions in graphene. *Nature* **2005**, *438*, 197–200. [CrossRef]

85. Novoselov, K.S.; Geim, A.K.; Morozov, S.V.; Jiang, D.; Zhang, Y.; Dubonos, S.V.; Grigorieva, I.V.; Firsov, A.A. Electric field effect in atomically thin carbon films. *Science* **2004**, *306*, 666–669. [CrossRef] [PubMed]

86. Wallbank, J.R.; Patel, A.; Mucha-Kruczynski, M.; Geim, A.K.; Fal'Ko, V. Generic miniband structure of graphene on a hexagonal substrate. *Phys. Rev. B* **2013**, *87*, 245408. [CrossRef]

87. Ambrosi, A.; Sasaki, T.; Pumera, M. Platelet Graphite Nanofibers for Electrochemical Sensing and Biosensing: The Influence of Graphene Sheet Orientation. *Chem.-Asian J.* **2010**, *5*, 266–271. [CrossRef]

88. Li, X.; Zhu, Y.; Cai, W.; Borysiak, M.; Han, B.; Chen, D.; Piner, R.D.; Colombo, L.; Ruoff, R.S. Transfer of Large-Area Graphene Films for High-Performance Transparent Conductive Electrodes. *Nano Lett.* **2009**, *9*, 4359–4363. [CrossRef]

89. Balandin, A.A.; Ghosh, S.; Bao, W.; Calizo, I.; Teweldebrhan, D.; Miao, F.; Lau, C.N. Superior Thermal Conductivity of Single-Layer Graphene. *Nano Lett.* **2008**, *8*, 902–907. [CrossRef]

90. Brownson, D.A.C.; Kampouris, D.K.; Banks, C.E. Graphene electrochemistry: Fundamental concepts through to prominent applications. *Chem. Soc. Rev.* **2012**, *41*, 6944–6976. [CrossRef]

91. Meng, F.; Lu, W.; Li, Q.; Byun, J.-H.; Oh, Y.; Chou, T.-W. Graphene-Based Fibers: A Review. *Adv. Mater.* **2015**, *27*, 5113–5131. [CrossRef] [PubMed]

92. Stankovich, S.; Dikin, D.A.; Dommett, G.H.B.; Kohlhaas, K.M.; Zimney, E.J.; Stach, E.A.; Piner, R.D.; Nguyen, S.T.; Ruoff, R.S. Graphene-based composite materials. *Nature* **2006**, *442*, 282–286. [CrossRef] [PubMed]

93. Stankovich, S.; Dikin, D.A.; Piner, R.D.; Kohlhaas, K.A.; Kleinhammes, A.; Jia, Y.; Wu, Y.; Nguyen, S.T.; Ruoff, R.S. Synthesis of graphene-based nanosheets via chemical reduction of exfoliated graphite oxide. *Carbon* **2007**, *45*, 1558–1565. [CrossRef]

94. Shateri-Khalilabad, M.; Yazdanshenas, M.E. Fabricating electroconductive cotton textiles using graphene. *Carbohydr. Polym.* **2013**, *96*, 190–195. [CrossRef]

95. Abdelkader, A.M.; Karim, N.; Vallés, C.; Afroj, S.; Novoselov, K.S.; Yeates, S.G. Ultraflexible and robust graphene supercapacitors printed on textiles for wearable electronics applications. *2D Mater.* **2017**, *4*, 035016. [CrossRef]

96. Karim, N.; Afroj, S.; Tan, S.; Novoselov, K.S.; Yeates, S.G. All Inkjet-Printed Graphene-Silver Composite Ink on Textiles for Highly Conductive Wearable Electronics Applications. *Sci. Rep.* **2019**, *9*, 1–10. [CrossRef]

97. Yu, G.; Hu, L.; Vosgueritchian, M.; Wang, H.; Xie, X.; McDonough, J.R.; Cui, X.; Cui, Y.; Bao, Z. Solution-Processed Graphene/MnO$_2$ Nanostructured Textiles for High-Performance Electrochemical Capacitors. *Nano Lett.* **2011**, *11*, 2905–2911. [CrossRef]

98. Molina, J.; Fernández, J.; Inés, J.C.; del Río, A.I.; Bonastre, J.; Cases, F. Electrochemical characterization of reduced graphene oxide-coated polyester fabrics. *Electrochim. Acta* **2013**, *93*, 44–52. [CrossRef]

99. Karim, N.; Afroj, S.; Tan, S.; He, P.; Fernando, A.; Carr, C.; Novoselov, K.S. Scalable Production of Graphene-Based Wearable E-Textiles. *ACS Nano* **2017**, *11*, 12266–12275. [CrossRef]

100. Chen, J.; Yao, B.; Li, C.; Shi, G. An improved Hummers method for eco-friendly synthesis of graphene oxide. *Carbon* **2013**, *64*, 225–229. [CrossRef]

101. Shateri-Khalilabad, M.; Yazdanshenas, M.E. Preparation of superhydrophobic electroconductive graphene-coated cotton cellulose. *Cellulose* **2013**, *20*, 963–972. [CrossRef]

102. Ramadoss, A.; Saravanakumar, B.; Kim, S.J. Thermally reduced graphene oxide-coated fabrics for flexible supercapacitors and self-powered systems. *Nano Energy* **2015**, *15*, 587–597. [CrossRef]

103. Yakubu, A.; Abbas, Z.; Danjumma, S.G. Graphene Synthesis by Chemical Vapour Deposition (CVD): A Review on Growth Mechanism and Techniques. *Int. J. Eng. Res.* **2019**, *8*, 15–26. [CrossRef]

104. Srivastava, S.K.; Shukla, A.; Vankar, V.; Kumar, V. Growth, structure and field emission characteristics of petal like carbon nano-structured thin films. *Thin Solid Films* **2005**, *492*, 124–130. [CrossRef]

105. Zhu, M.; Wang, J.; Outlaw, R.A.; Hou, K.; Manos, D.M.; Holloway, B.C. Synthesis of carbon nanosheets and carbon nanotubes by radio frequency plasma enhanced chemical vapor deposition. *Diam. Relat. Mater.* **2007**, *16*, 196–201. [CrossRef]

106. Ghasemi, S.; Hosseini, S.R.; Asen, P. Preparation of graphene/nickel-iron hexacyanoferrate coordination polymer nanocomposite for electrochemical energy storage. *Electrochim. Acta* **2015**, *160*, 337–346. [CrossRef]

107. Ji, L.; Meduri, P.; Agubra, V.; Xiao, X.; Alcoutlabi, M. Graphene-Based Nanocomposites for Energy Storage. *Adv. Energy Mater.* **2016**, *6*, 1502159. [CrossRef]

108. Mahmood, N.; Zhang, C.; Yin, H.; Hou, Y. Graphene-based nanocomposites for energy storage and conversion in lithium batteries, supercapacitors and fuel cells. *J. Mater. Chem. A* **2013**, *2*, 15–32. [CrossRef]

109. Yousefi, N.; Sun, X.; Lin, X.; Shen, X.; Jia, J.; Zhang, B.; Tang, B.; Chan, M.; Kim, J.-K. Highly Aligned Graphene/Polymer Nanocomposites with Excellent Dielectric Properties for High-Performance Electromagnetic Interference Shielding. *Adv. Mater.* **2014**, *26*, 5480–5487. [CrossRef]

110. Abbasi, H.; Antunes, M.; Velasco, J.I. Recent advances in carbon-based polymer nanocomposites for electromagnetic interference shielding. *Prog. Mater. Sci.* **2019**, *103*, 319–373. [CrossRef]

111. Duan, F.; Liao, Y.; Zeng, Z.; Jin, H.; Zhou, L.; Zhang, Z.; Su, Z. Graphene-based nanocomposite strain sensor response to ultrasonic guided waves. *Compos. Sci. Technol.* **2019**, *174*, 42–49. [CrossRef]

112. Stoller, M.D.; Murali, S.; Quarles, N.; Zhu, Y.; Potts, J.R.; Zhu, X.; Ha, H.-W.; Ruoff, R.S. Activated graphene as a cathode material for Li-ion hybrid supercapacitors. *Phys. Chem. Chem. Phys.* **2012**, *14*, 3388–3391. [CrossRef] [PubMed]

113. Zheng, C.; Zhou, X.; Cao, H.; Wang, G.; Liu, Z. Synthesis of porous graphene/activated carbon composite with high packing density and large specific surface area for supercapacitor electrode material. *J. Power Sources* **2014**, *258*, 290–296. [CrossRef]

114. Li, X.; Tang, Y.; Song, J.; Yang, W.; Wang, M.; Zhu, C.; Zhao, W.; Zheng, J.; Lin, Y. Self-supporting activated carbon/carbon nanotube/reduced graphene oxide flexible electrode for high performance supercapacitor. *Carbon* **2018**, *129*, 236–244. [CrossRef]

115. Wu, Z.-S.; Zhou, G.; Yin, L.-C.; Ren, W.; Li, F.; Cheng, H.-M. Graphene/metal oxide composite electrode materials for energy storage. *Nano Energy* **2011**, *1*, 107–131. [CrossRef]

116. Xu, H.; Chen, H.; Lai, H.; Li, Z.; Dong, X.; Cai, S.; Chu, X.; Gao, C. Capacitive charge storage enables an ultrahigh cathode capacity in aluminum-graphene battery. *J. Energy Chem.* **2019**, *45*, 40–44. [CrossRef]

117. Zhao, X.; Hayner, C.M.; Kung, M.C.; Kung, H.H. In-Plane Vacancy-Enabled High-Power Si-Graphene Composite Electrode for Lithium-Ion Batteries. *Adv. Energy Mater.* **2011**, *1*, 1079–1084. [CrossRef]

118. Shi, Q.; Li, J.; Hou, C.; Shao, Y.; Zhang, Q.; Li, Y.; Wang, H. A remote controllable fiber-type near-infrared light-responsive actuator. *Chem. Commun.* **2017**, *53*, 11118–11121. [CrossRef]

119. Cheng, H.; Liu, J.; Zhao, Y.; Hu, C.; Zhang, Z.; Chen, N.; Jiang, L.; Qu, L. Graphene Fibers with Predetermined Deformation as Moisture-Triggered Actuators and Robots. *Angew. Chem. Int. Ed.* **2013**, *52*, 10482–10486. [CrossRef]

120. Qiao, J.; Di, J.; Zhou, S.; Jin, K.; Zeng, S.; Li, N.; Fang, S.; Song, Y.; Li, M.; Baughman, R.H.; et al. Large-Stroke Electrochemical Carbon Nanotube/Graphene Hybrid Yarn Muscles. *Small* **2018**, *14*, e1801883. [CrossRef]

121. Sasikala, S.P.; Lee, K.E.; Lim, J.; Lee, H.J.; Koo, S.H.; Kim, I.H.; Jung, H.J.; Kim, S.O. Interface-Confined High Crystalline Growth of Semiconducting Polymers at Graphene Fibers for High-Performance Wearable Supercapacitors. *ACS Nano* **2017**, *11*, 9424–9434. [CrossRef]

122. Meng, Y.; Zhao, Y.; Hu, C.; Cheng, H.; Hu, Y.; Zhang, Z.; Shi, G.; Qu, L. All-Graphene Core-Sheath Microfibers for All-Solid-State, Stretchable Fibriform Supercapacitors and Wearable Electronic Textiles. *Adv. Mater.* **2013**, *25*, 2326–2331. [CrossRef]

123. Wang, H.; Sun, K.; Tao, F.; Stacchiola, D.J.; Hu, Y.H. 3D Honeycomb-Like Structured Graphene and Its High Efficiency as a Counter-Electrode Catalyst for Dye-Sensitized Solar Cells. *Angew. Chem. Int. Ed.* **2013**, *52*, 9210–9214. [CrossRef] [PubMed]

124. Yang, Z.; Sun, H.; Chen, T.; Qiu, L.; Luo, Y.; Peng, H. Photovoltaic Wire Derived from a Graphene Composite Fiber Achieving an 8.45 % Energy Conversion Efficiency. *Angew. Chem.* **2013**, *125*, 7693–7696. [CrossRef]

125. Prasai, D.; Tuberquia, J.C.; Harl, R.R.; Jennings, G.K.; Bolotin, K.I. Graphene: Corrosion-Inhibiting Coating. *ACS Nano* **2012**, *6*, 1102–1108. [CrossRef] [PubMed]

126. Hyun, W.J.; Park, O.O.; Chin, B.D. Foldable Graphene Electronic Circuits Based on Paper Substrates. *Adv. Mater.* **2013**, *25*, 4729–4734. [CrossRef]

127. Bonanni, A.; Pumera, M. Graphene Platform for Hairpin-DNA-Based Impedimetric Genosensing. *ACS Nano* **2011**, *5*, 2356–2361. [CrossRef]

128. Kasry, A.; Kuroda, M.A.; Martyna, G.J.; Tulevski, G.S.; Bol, A.A. Chemical Doping of Large-Area Stacked Graphene Films for Use as Transparent, Conducting Electrodes. *ACS Nano* **2010**, *4*, 3839–3844. [CrossRef]

129. De Arco, L.G.; Zhang, Y.; Schlenker, C.W.; Ryu, K.; Thompson, M.; Zhou, C. Continuous, Highly Flexible, and Transparent Graphene Films by Chemical Vapor Deposition for Organic Photovoltaics. *ACS Nano* **2010**, *4*, 2865–2873. [CrossRef]

130. Wang, H.; Cui, L.-F.; Yang, Y.; Sanchez Casalongue, H.; Robinson, J.T.; Liang, Y.; Cui, Y.; Dai, H. $Mn_3O_4-$Graphene Hybrid as a High-Capacity Anode Material for Lithium Ion Batteries. *J. Am. Chem. Soc.* **2010**, *132*, 13978–13980. [CrossRef]

131. Ang, P.K.; Chen, W.; Wee, A.T.S.; Loh, K.P. Solution-Gated Epitaxial Graphene as pH Sensor. *J. Am. Chem. Soc.* **2008**, *130*, 14392–14393. [CrossRef] [PubMed]

132. Dong, X.; Shi, Y.; Huang, W.; Chen, P.; Li, L.-J. Electrical Detection of DNA Hybridization with Single-Base Specificity Using Transistors Based on CVD-Grown Graphene Sheets. *Adv. Mater.* **2010**, *22*, 1649–1653. [CrossRef]

133. Patel, P.C.; Vasavada, D.A.; Mankodi, H.R. Applications of electrically conductive yarns in technical textiles. In Proceedings of the 2012 IEEE International Conference on Power System Technology (POWERCON), Auckland, New Zealand, 30 October–2 November 2012; pp. 1–6. [CrossRef]

134. Wang, L.; Wang, X.; Lin, T. 6—Conductive coatings for textiles. In *Smart Textile Coatings and Laminates*; Smith, W.C., Ed.; Woodhead Publishing: Cambridge, UK, 2010; pp. 155–188. [CrossRef]

135. Irwin, M.D.; Roberson, D.A.; Olivas, R.I.; Wicker, R.B.; Macdonald, E. Conductive polymer-coated threads as electrical interconnects in e-textiles. *Fibers Polym.* **2011**, *12*, 904–910. [CrossRef]

136. Pawlak, R.; Lebioda, M.; Tomczyk, M.; Rymaszewski, J.; Korzeniewska, E.; Walczak, M. Modelling and applications of conductive elements on textile materials. *COMPEL-Int. J. Comput. Math. Electr. Electron. Eng.* **2018**, *37*, 1645–1656. [CrossRef]

137. Shahidi, S.; Moazzenchi, B.; Ghoranneviss, M. A review-application of physical vapor deposition (PVD) and related methods in the textile industry. *Eur. Phys. J. Appl. Phys.* **2015**, *71*, 31302. [CrossRef]

138. Liu, J.L.; Bashir, S. *Advanced Nanomaterials and Their Applications in Renewable Energy*; Elsevier: Amsterdam, The Netherlands, 2015. [CrossRef]

139. Filho, J.M.C.D.S.; Ermakov, V.A.; Marques, F.C. Perovskite Thin Film Synthesised from Sputtered Lead Sulphide. *Sci. Rep.* **2018**, *8*, 1–8. [CrossRef]

140. Ostroverkhova, O. *Handbook of Organic Materials for Electronic and Photonic Devices*, 2nd ed.; Woodhead Publishing: Cambridge, UK, 2019. [CrossRef]

141. Pawlak, R.; Korzeniewska, E.; Koneczny, C.; Hałgas, B. Properties Of Thin Metal Layers Deposited On Textile Composites By Using The Pvd Method For Textronic Applications. *Autex Res. J.* **2017**, *17*, 229–237. [CrossRef]

142. Miśkiewicz, P.; Frydrych, I.; Cichocka, A. Application of Physical Vapor Deposition in Textile Industry. *Autex Res. J.* **2022**, *22*, 42–54. [CrossRef]

143. Shishkovsky, I.; Lebedev, P. 3—Chemical and physical vapor deposition methods for nanocoatings. In *Nanocoatings and Ultra-Thin Films*; Makhlouf, A.S.H., Tiginyanu, I., Eds.; Woodhead Publishing: Cambridge, UK, 2011; pp. 57–77. [CrossRef]

144. Mattox, D.M. *Handbook of Physical Vapor Deposition (PVD) Processing*, 2nd ed.; Elsevier: Amsterdam, The Netherlands, 2010.

145. Silva, N.L.; Gonçalves, L.M.; Carvalho, H. Deposition of conductive materials on textile and polymeric flexible substrates. *J. Mater. Sci. Mater. Electron.* **2012**, *24*, 635–643. [CrossRef]

146. Jilani, A.; Abdel-Wahab, M.S.; Hammad, A.H. Advance Deposition Techniques for Thin Film and Coating. In *Modern Technologies for Creating the Thin-Film Systems and Coatings*; Nikitenkov, N.N., Ed.; IntechOpen: London, UK, 2017; pp. 137–149. [CrossRef]

147. Aghamiri, S.; Rabiee, N.; Ahmadi, S.; Rabiee, M.; Bagherzadeh, M.; Karimi, M. Microfluidic devices: Synthetic approaches. In *Biomedical Applications of Microfluidic Devices*; Academic Press: London, UK, 2021; pp. 23–36. [CrossRef]

148. Krishna, J.; Perumal, A.S.; Khan, I.; Chelliah, R.; Wei, S.; Swamidoss, C.M.A.; Oh, D.-H.; Bharathiraja, B. Synthesis of nanomaterials for biofuel and bioenergy applications. In *Nanomaterials*; Academic Press: London, UK, 2021; pp. 97–165. [CrossRef]

149. Renken, A.; Kiwi-Minsker, L. Microstructured catalytic reactors. In *Advances in Catalysis*; Academic Press: Amsterdam, The Netherlands, 2010; Volume 53, pp. 47–122. [CrossRef]

150. Vančo, M.; Krmela, J.; Pešlová, F. The Use of PVD Coating on Natural Textile Fibers. *Procedia Eng.* **2016**, *136*, 341–345. [CrossRef]

151. Esen, M.; Ilhan, I.; Karaaslan, M.; Esen, R. Investigation of electromagnetic and ultraviolet properties of nano-metal-coated textile surfaces. *Appl. Nanosci.* **2019**, *10*, 551–561. [CrossRef]

152. Abegunde, O.O.; Akinlabi, E.T.; Oladijo, O.P.; Akinlabi, S.; Ude, A.U. Overview of thin film deposition techniques. *AIMS Mater. Sci.* **2019**, *6*, 174–199. [CrossRef]

153. Park, J.; Lee, J.W.; Choi, H.J.; Jang, W.G.; Kim, T.S.; Suh, D.S.; Jeong, H.Y.; Chang, S.Y.; Roh, J.C.; Yoo, C.S.; et al. Electromagnetic interference shielding effectiveness of sputtered NiFe/Cu multi-layer thin film at high frequencies. *Thin Solid Films* **2019**, *677*, 130–136. [CrossRef]

154. Jang, S.; Cho, J.; Jeong, K.; Cho, G. Exploring possibilities of ECG electrodes for bio-monitoring smartwear with Cu sputtered fabrics. In Proceedings of the International Conference on Human-Computer Interaction, Beijing, China, 22–27 July 2007; pp. 1130–1137.

155. Wang, K.; Huang, Y.; Wang, M.; Yu, M.; Zhu, Y.; Wu, J. PVD amorphous carbon coated 3D NiCo$_2$O$_4$ on carbon cloth as flexible electrode for both sodium and lithium storage. *Carbon* **2017**, *125*, 375–383. [CrossRef]

156. Zhu, Y.; Huang, Y.; Wang, M.; Wang, K.; Yu, M.; Chen, X.; Zhang, Z. Novel carbon coated core-shell heterostructure NiCo2O4@NiO grown on carbon cloth as flexible lithium-ion battery anodes. *Ceram. Int.* **2018**, *44*, 21690–21698. [CrossRef]

157. Choy, K. Chemical vapour deposition of coatings. *Prog. Mater. Sci.* **2003**, *48*, 57–170. [CrossRef]

158. de Lodyguine, A. Illuminesenz for Incandescent Lamps. U.S. Patent US575002A, 12 January 1897. Available online: https://patents.google.com/patent/US575002A/en (accessed on 30 August 2022).

159. Malinauskas, A. Chemical deposition of conducting polymers. *Polymer* **2001**, *42*, 3957–3972. [CrossRef]

160. Tan, S.N.; Ge, H. Investigation into vapour-phase formation of polypyrrole. *Polymer* **1996**, *37*, 965–968. [CrossRef]

161. Dall'Acqua, L.; Tonin, C.; Peila, R.; Ferrero, F.; Catellani, M. Performances and properties of intrinsic conductive cellulose–polypyrrole textiles. *Synth. Met.* **2004**, *146*, 213–221. [CrossRef]

162. Xia, Y.; Lu, Y. Fabrication and properties of conductive conjugated polymers/silk fibroin composite fibers. *Compos. Sci. Technol.* **2008**, *68*, 1471–1479. [CrossRef]

163. Gregory, R.; Kimbrell, W.; Kuhn, H. Electrically Conductive Non-Metallic Textile Coatings. *J. Coat. Fabr.* **1991**, *20*, 167–175. [CrossRef]

164. Jang, J.; Chang, M.; Yoon, H. Chemical Sensors Based on Highly Conductive Poly(3,4-ethylenedioxythiophene) Nanorods. *Adv. Mater.* **2005**, *17*, 1616–1620. [CrossRef]

165. Tenhaeff, W.E.; Gleason, K.K. Initiated and Oxidative Chemical Vapor Deposition of Polymeric Thin Films: iCVD and oCVD. *Adv. Funct. Mater.* **2008**, *18*, 979–992. [CrossRef]

166. Yang, X.; Shang, S.; Li, L.; Tao, X.-M.; Yan, F. Vapor phase polymerization of 3,4-ethylenedioxythiophene on flexible substrate and its application on heat generation. *Polym. Adv. Technol.* **2009**, *22*, 1049–1055. [CrossRef]

167. Bashir, T.; Skrifvars, M.; Persson, N.-K. Synthesis of high performance, conductive PEDOT-coated polyester yarns by OCVD technique. *Polym. Adv. Technol.* **2011**, *23*, 611–617. [CrossRef]

168. Hyde, K.; Dong, H.; Hinestroza, J. Effect of surface cationization on the conformal deposition of polyelectrolytes over cotton fibers. *Cellulose* **2007**, *14*, 615–623. [CrossRef]

169. Wang, Y.; Wang, W.; Qi, Q.; Xu, N.; Yu, D. Layer-by-layer assembly of PDMS-coated nickel ferrite/multiwalled carbon nanotubes/cotton fabrics for robust and durable electromagnetic interference shielding. *Cellulose* **2020**, *27*, 2829–2845. [CrossRef]

170. Parvinzadeh Gashti, M.; Alimohammadi, F.; Song, G.; Kiumarsi, A. Characterization of nanocomposite coatings on textiles: A brief review on Microscopic technology. *Curr. Microsc. Contrib. Adv. Sci. Technol.* **2012**, *2*, 1424–1437.

171. Gulrajani, M.; Gupta, D. Emerging techniques for functional finishing of textiles. *Indian J. Fibre Text Res.* **2011**, *36*, 388–397.

172. Parsons, G.N.; Atanasov, S.E.; Dandley, E.C.; Devine, C.K.; Gong, B.; Jur, J.S.; Lee, K.; Oldham, C.J.; Peng, Q.; Spagnola, J.C.; et al. Mechanisms and reactions during atomic layer deposition on polymers. *Coord. Chem. Rev.* **2013**, *257*, 3323–3331. [CrossRef]

173. Brozena, A.H.; Oldham, C.J.; Parsons, G.N. Atomic layer deposition on polymer fibers and fabrics for multifunctional and electronic textiles. *J. Vac. Sci. Technol. A Vac. Surfaces Films* **2016**, *34*, 010801. [CrossRef]

174. Saetia, K.; Schnorr, J.M.; Mannarino, M.M.; Kim, S.Y.; Rutledge, G.C.; Swager, T.M.; Hammond, P.T. Spray-Layer-by-Layer Carbon Nanotube/Electrospun Fiber Electrodes for Flexible Chemiresistive Sensor Applications. *Adv. Funct. Mater.* **2013**, *24*, 492–502. [CrossRef]

175. Xu, D.; Yang, R. Efficient preparation and characterization of paraffin-based microcapsules by emulsion polymerization. *J. Appl. Polym. Sci.* **2019**, *136*, 47552. [CrossRef]

176. Tian, M.; Du, M.; Qu, L.; Chen, S.; Zhu, S.; Han, G. Electromagnetic interference shielding cotton fabrics with high electrical conductivity and electrical heating behavior via layer-by-layer self-assembly route. *RSC Adv.* **2017**, *7*, 42641–42652. [CrossRef]

177. Shakir, I.; Ali, Z.; Bae, J.; Park, J.; Kang, D.J. Layer by layer assembly of ultrathin $V_2O_5$ anchored MWCNTs and graphene on textile fabrics for fabrication of high energy density flexible supercapacitor electrodes. *Nanoscale* **2014**, *6*, 4125–4130. [CrossRef]

178. Ahmed, H.B.; Emam, H.E. Layer by layer assembly of nanosilver for high performance cotton fabrics. *Fibers Polym.* **2016**, *17*, 418–426. [CrossRef]

179. Prakash, S.; Yeom, J. Chapter 4—Advanced Fabrication Methods and Techniques. In *Nanofluidics and Microfluidics*; William Andrew Publishing: Waltham, MA, USA, 2014; pp. 87–170. [CrossRef]

180. Shang, S.; Zeng, W. 4—Conductive nanofibres and nanocoatings for smart textiles. In *Multidisciplinary Know-How for Smart-Textiles Developers*; Kirstein, T., Ed.; Woodhead Publishing: Cambridge, UK, 2013; pp. 92–128. [CrossRef]

181. Torabinejad, V.; Aliofkhazraei, M.; Assareh, S.; Allahyarzadeh, M.H.; Rouhaghdam, A.S. Electrodeposition of Ni-Fe alloys, composites, and nano coatings—A review. *J. Alloy. Compd.* **2017**, *691*, 841–859. [CrossRef]

182. Zhitomirsky, I. Cathodic electrodeposition of ceramic and organoceramic materials. Fundamental aspects. *Adv. Colloid Interface Sci.* **2002**, *97*, 279–317. [CrossRef]

183. Lincot, D. Electrodeposition of semiconductors. *Thin Solid Films* **2005**, *487*, 40–48. [CrossRef]

184. Bicelli, L.; Bozzini, B.; Mele, C.; D'Urzo, L. A Review of Nanostructural Aspects of Metal Electrodeposition. *Int. J. Electrochem. Sci.* **2008**, *3*, 356–408.

185. Biswal, H.J.; Vundavilli, P.R.; Gupta, A. Perspective—Electrodeposition of Graphene Reinforced Metal Matrix Composites for Enhanced Mechanical and Physical Properties: A Review. *J. Electrochem. Soc.* **2020**, *167*, 146501. [CrossRef]

186. Wang, Y.; Liu, A.; Han, Y.; Li, T. Sensors based on conductive polymers and their composites: A review. *Polym. Int.* **2019**, *69*, 7–17. [CrossRef]

187. Wang, Y.; Zhang, L.; Hou, H.; Xu, W.; Duan, G.; He, S.; Liu, K.; Jiang, S. Recent progress in carbon-based materials for supercapacitor electrodes: A review. *J. Mater. Sci.* **2021**, *56*, 173–200. [CrossRef]

188. Zhang, Q.-Z.; Zhang, D.; Miao, Z.-C.; Zhang, X.-L.; Chou, S.-L. Research Progress in $MnO_2$-Carbon Based Supercapacitor Electrode Materials. *Small* **2018**, *14*, 1702883. [CrossRef]

189. Chen, H.; Wei, Z.; Zheng, X.; Yang, S. A scalable electrodeposition route to the low-cost, versatile and controllable fabrication of perovskite solar cells. *Nano Energy* **2015**, *15*, 216–226. [CrossRef]

190. Sreedeviamma, D.K.; Remadevi, A.; Sruthi, C.V.; Pillai, S.; Peethambharan, S.K. Nickel electrodeposited textiles as wearable radar invisible fabrics. *J. Ind. Eng. Chem.* **2020**, *88*, 196–206. [CrossRef]

191. Darvishzadeh, A.; Nasouri, K. Manufacturing, modeling, and optimization of nickel-coated carbon fabric for highly efficient EMI shielding. *Surf. Coat. Technol.* **2021**, *409*, 126957. [CrossRef]

192. Zhang, H.; Wang, S.; Tian, Y.; Liu, Y.; Wen, J.; Huang, Y.; Hang, C.; Zheng, Z.; Wang, C. Electrodeposition fabrication of Cu@Ni core shell nanowire network for highly stable transparent conductive films. *Chem. Eng. J.* **2020**, *390*, 124495. [CrossRef]

193. Habib, M.A.; Rahman, M. Analysis of Electrolyte Flow in Localized Electrochemical Deposition. *Procedia Eng.* **2013**, *56*, 766–771. [CrossRef]

194. Lu, X.; Shang, W.; Chen, G.; Wang, H.; Tan, P.; Deng, X.; Song, H.; Xu, Z.; Huang, J.; Zhou, X. Environmentally Stable, Highly Conductive, and Mechanically Robust Metallized Textiles. *ACS Appl. Electron. Mater.* **2021**, *3*, 1477–1488. [CrossRef]

195. Qi, K.; Hou, R.; Zaman, S.; Qiu, Y.; Xia, B.Y.; Duan, H. Construction of Metal–Organic Framework/Conductive Polymer Hybrid for All-Solid-State Fabric Supercapacitor. *ACS Appl. Mater. Interfaces* **2018**, *10*, 18021–18028. [CrossRef] [PubMed]

196. Hu, L.; Chen, W.; Xie, X.; Liu, N.; Yang, Y.; Wu, H.; Yao, Y.; Pasta, M.; Alshareef, H.N.; Cui, Y. Symmetrical $MnO_2$–Carbon Nanotube–Textile Nanostructures for Wearable Pseudocapacitors with High Mass Loading. *ACS Nano* **2011**, *5*, 8904–8913. [CrossRef] [PubMed]

197. Zhang, J.; Wang, Y.; Zang, J.; Xin, G.; Yuan, Y.; Qu, X. Electrophoretic deposition of $MnO_2$-coated carbon nanotubes on a graphite sheet as a flexible electrode for supercapacitors. *Carbon* **2012**, *50*, 5196–5202. [CrossRef]

198. Qiu, Y.; Xu, P.; Guo, B.; Cheng, Z.; Fan, H.; Yang, M.; Yang, X.; Li, J. Electrodeposition of manganese dioxide film on activated carbon paper and its application in supercapacitors with high rate capability. *RSC Adv.* **2014**, *4*, 64187–64192. [CrossRef]

199. Kim, Y.K.; Hwang, S.-H.; Kim, S.; Park, H.; Lim, S.K. ZnO nanostructure electrodeposited on flexible conductive fabric: A flexible photo-sensor. *Sens. Actuators B Chem.* **2017**, *240*, 1106–1113. [CrossRef]

200. Rosa-Ortiz, S.M.; Takshi, A. Copper Electrodeposition by Hydrogen Evolution Assisted Electroplating (HEA) for Wearable Electronics. In Proceedings of the 2020 Pan Pacific Microelectronics Symposium (Pan Pacific), Big Island, HI, USA, 10–13 February 2020; pp. 1–5. [CrossRef]

201. Chen, H.; Liao, F.; Yuan, Z.; Han, X.; Xu, C. Simple and fast fabrication of conductive silver coatings on carbon fabrics via an electroless plating technique. *Mater. Lett.* **2017**, *196*, 205–208. [CrossRef]

202. Cao, S.; Pedraza, A.; Allard, L. Laser-induced microstructural changes and decomposition of aluminum nitride. *J. Mater. Res.* **1995**, *10*, 54–62. [CrossRef]

203. Staňo, M.; Fruchart, O. Magnetic nanowires and nanotubes. In *Handbook of Magnetic Materials*; Elsevier: Amsterdam, The Netherlands, 2018; Volume 27, pp. 155–267. [CrossRef]

204. Lahiri, A.; Pulletikurthi, G.; Endres, F. A Review on the Electroless Deposition of Functional Materials in Ionic Liquids for Batteries and Catalysis. *Front. Chem.* **2019**, *7*, 85. [CrossRef]

205. Root, W.; Aguiló-Aguayo, N.; Pham, T.; Bechtold, T. Conductive layers through electroless deposition of copper on woven cellulose lyocell fabrics. *Surf. Coat. Technol.* **2018**, *348*, 13–21. [CrossRef]

206. Gan, X.; Wu, Y.; Liu, L.; Shen, B.; Hu, W. Electroless plating of Cu–Ni–P alloy on PET fabrics and effect of plating parameters on the properties of conductive fabrics. *J. Alloy. Compd.* **2008**, *455*, 308–313. [CrossRef]

207. Lu, Y.; Jiang, S.; Huang, Y. Ultrasonic-assisted electroless deposition of Ag on PET fabric with low silver content for EMI shielding. *Surf. Coat. Technol.* **2010**, *204*, 2829–2833. [CrossRef]

208. Montazer, M.; Allahyarzadeh, V. Electroless Plating of Silver Nanoparticles/Nanolayer on Polyester Fabric Using $AgNO_3$/NaOH and Ammonia. *Ind. Eng. Chem. Res.* **2013**, *52*, 8436–8444. [CrossRef]

209. Liu, H.; Zhu, L.-L.; He, Y.; Cheng, B.-W. A novel method for fabricating elastic conductive polyurethane filaments by in-situ reduction of polydopamine and electroless silver plating. *Mater. Des.* **2017**, *113*, 254–263. [CrossRef]

210. Lin, X.; Wu, M.; Zhang, L.; Wang, D. Superior Stretchable Conductors by Electroless Plating of Copper on Knitted Fabrics. *ACS Appl. Electron. Mater.* **2019**, *1*, 397–406. [CrossRef]

211. Guo, R.H.; Jiang, S.Q.; Yuen, C.W.M.; Ng, M.C.F. An alternative process for electroless copper plating on polyester fabric. *J. Mater. Sci. Mater. Electron.* **2008**, *20*, 33–38. [CrossRef]

212. Kim, E.-Y.; Kong, J.-S.; An, S.-K.; Kim, H.-D. Surface modification of polymers and improvement of the adhesion between evaporated copper metal film and a polymer. I. Chemical modification of PET. *J. Adhes. Sci. Technol.* **2000**, *14*, 1119–1130. [CrossRef]

213. Lu, Y. Electroless copper plating on 3-mercaptopropyltriethoxysilane modified PET fabric challenged by ultrasonic washing. *Appl. Surf. Sci.* **2009**, *255*, 8430–8434. [CrossRef]

214. Paquin, F.; Rivnay, J.; Salleo, A.; Stingelin, N.; Silva-Acuña, C. Multi-phase microstructures drive exciton dissociation in neat semicrystalline polymeric semiconductors. *J. Mater. Chem. C* **2015**, *3*, 10715–10722. [CrossRef]

215. Ali, A.; Baheti, V.; Vik, M.; Militky, J. Copper electroless plating of cotton fabrics after surface activation with deposition of silver and copper nanoparticles. *J. Phys. Chem. Solids* **2019**, *137*, 109181. [CrossRef]

216. Li, X.; Li, Y.; Guan, T.; Xu, F.; Sun, J. Durable, Highly Electrically Conductive Cotton Fabrics with Healable Superamphiphobicity. *ACS Appl. Mater. Interfaces* **2018**, *10*, 12042–12050. [CrossRef]

217. Hassan, Z.; Atalay, O.; Kalaoglu, F. Conductive cotton fabric using laser pre-treatment and electroless plating. *J. Text. Inst.* **2021**, *113*, 737–747. [CrossRef]

218. Grothe, J.; Kaskel, S.; Leuteritz, A. Nanocomposites and hybrid materials. In *Polymer Science: A Comprehensive Reference*; 10 Volume Set; Elsevier: Amsterdam, The Netherlands, 2012; pp. 177–209. [CrossRef]

219. Maity, S.; Chatterjee, A. Conductive polymer-based electro-conductive textile composites for electromagnetic interference shielding: A review. *J. Ind. Text.* **2016**, *47*, 2228–2252. [CrossRef]

220. Liu, T.; Zhang, J.; Han, W.; Zhang, J.; Ding, G.; Dong, S.; Cui, G. Review—In Situ Polymerization for Integration and Interfacial Protection Towards Solid State Lithium Batteries. *J. Electrochem. Soc.* **2020**, *167*, 070527. [CrossRef]

221. Ansari, M.O.; Khan, M.M.; Ansari, S.A.; Raju, K.; Lee, J.; Cho, M.H. Enhanced Thermal Stability under DC Electrical Conductivity Retention and Visible Light Activity of Ag/$TiO_2$@Polyaniline Nanocomposite Film. *ACS Appl. Mater. Interfaces* **2014**, *6*, 8124–8133. [CrossRef]

222. Hong, K.H.; Oh, K.W.; Kang, T.J. Preparation and properties of electrically conducting textiles byin situ polymerization of poly(3,4-ethylenedioxythiophene). *J. Appl. Polym. Sci.* **2005**, *97*, 1326–1332. [CrossRef]

223. Grishina, T.R. The effect of the table salt substitute sanasol on arterial pressure, water-salt metabolism and kidney functions in experimental pathology of circulatory homeostasis. *Eksp. Klin. Farmakol.* **1992**, *55*, 21–24.

224. Dey, M.; Doumenc, F.; Guerrier, B. Numerical simulation of dip-coating in the evaporative regime. *Eur. Phys. J. E* **2016**, *39*, 19. [CrossRef]

225. Gaulding, E.A.; Diroll, B.T.; Goodwin, E.D.; Vrtis, Z.J.; Kagan, C.R.; Murray, C.B. Deposition of Wafer-Scale Single-Component and Binary Nanocrystal Superlattice Thin Films Via Dip-Coating. *Adv. Mater.* **2015**, *27*, 2846–2851. [CrossRef]

226. Ceratti, D.R.; Louis, B.; Paquez, X.; Faustini, M.; Grosso, D. A New Dip Coating Method to Obtain Large-Surface Coatings with a Minimum of Solution. *Adv. Mater.* **2015**, *27*, 4958–4962. [CrossRef]

227. Roland, S.; Pellerin, C.; Bazuin, C.G.; Prud'Homme, R.E. Evolution of Small Molecule Content and Morphology with Dip-Coating Rate in Supramolecular PS–P4VP Thin Films. *Macromolecules* **2012**, *45*, 7964–7972. [CrossRef]

228. Jittavanich, K.; Clemons, C.; Kreider, K.; Aljarrah, M.; Evans, E.; Young, G. Modeling, simulation and fabrication of coated structures using the dip coating technique. *Chem. Eng. Sci.* **2010**, *65*, 6169–6180. [CrossRef]

229. Tang, X.; Yan, X. Dip-coating for fibrous materials: Mechanism, methods and applications. *J. Sol-Gel Sci. Technol.* **2016**, *81*, 378–404. [CrossRef]

230. He, S.; Xin, B.; Chen, Z.; Liu, Y. Flexible and highly conductive Ag/G-coated cotton fabric based on graphene dipping and silver magnetron sputtering. *Cellulose* **2018**, *25*, 3691–3701. [CrossRef]

231. Alongi, J.; Ciobanu, M.; Tata, J.; Carosio, F.; Malucelli, G. Thermal stability and flame retardancy of polyester, cotton, and relative blend textile fabrics subjected to sol-gel treatments. *J. Appl. Polym. Sci.* **2010**, *119*, 1961–1969. [CrossRef]

232. Gorenšek, M.; Recelj, P. Nanosilver Functionalized Cotton Fabric. *Text. Res. J.* **2007**, *77*, 138–141. [CrossRef]

233. Abidi, N.; Hequet, E.; Tarimala, S.; Dai, L.L. Cotton fabric surface modification for improved UV radiation protection using sol–gel process. *J. Appl. Polym. Sci.* **2007**, *104*, 111–117. [CrossRef]

234. Mahltig, B.; Textor, T. Combination of silica sol and dyes on textiles. *J. Sol-Gel Sci. Technol.* **2006**, *39*, 111–118. [CrossRef]

235. Schramm, C.; Binder, W.; Tessadri, R. Durable Press Finishing of Cotton Fabric with 1,2,3,4-Butanetetracarboxylic Acid and TEOS/GPTMS. *J. Sol-Gel Sci. Technol.* **2004**, *29*, 155–165. [CrossRef]

236. Kampeerapappun, P.; Visatchok, K.; Wangarsa, D. Preparation and properties of superhydrophobic cotton fabrics. *J. Met. Mater. Miner.* **2010**, *20*, 79–83.

237. Nasirizadeh, N.; Dehghani, M.; Yazdanshenas, M.E. Preparation of hydrophobic and conductive cotton fabrics using multi-wall carbon nanotubes by the sol–gel method. *J. Sol-Gel Sci. Technol.* **2014**, *73*, 14–21. [CrossRef]

238. Kwon, S.; Kim, W.; Kim, H.; Choi, S.; Park, B.-C.; Kang, S.-H.; Choi, K.C. High Luminance Fiber-Based Polymer Light-Emitting Devices by a Dip-Coating Method. *Adv. Electron. Mater.* **2015**, *1*, 1500103. [CrossRef]

239. Pu, D.; Zhou, W.; Li, Y.; Chen, J.; Chen, J.; Zhang, H.; Mi, B.; Wang, L.; Ma, Y. Order-enhanced silver nanowire networks fabricated by two-step dip-coating as polymer solar cell electrodes. *RSC Adv.* **2015**, *5*, 100725–100729. [CrossRef]

240. Liu, L.; Chen, W.; Zhang, H.; Wang, Q.; Guan, F.; Yu, Z. Flexible and Multifunctional Silk Textiles with Biomimetic Leaf-Like MXene/Silver Nanowire Nanostructures for Electromagnetic Interference Shielding, Humidity Monitoring, and Self-Derived Hydrophobicity. *Adv. Funct. Mater.* **2019**, *29*, 1905197. [CrossRef]

241. Zhang, S.; Li, Y.; Pan, N. Graphene based supercapacitor fabricated by vacuum filtration deposition. *J. Power Sources* **2012**, *206*, 476–482. [CrossRef]

242. Naghdi, S.; Rhee, K.Y.; Hui, D.; Park, S.J. A Review of Conductive Metal Nanomaterials as Conductive, Transparent, and Flexible Coatings, Thin Films, and Conductive Fillers: Different Deposition Methods and Applications. *Coatings* **2018**, *8*, 278. [CrossRef]

243. Gong, F.; Meng, C.; He, J.; Dong, X. Fabrication of highly conductive and multifunctional polyester fabrics by spray-coating with PEDOT:PSS solutions. *Prog. Org. Coat.* **2018**, *121*, 89–96. [CrossRef]

244. Zhang, M.; Wang, C.; Wang, Q.; Jian, M.; Zhang, Y. Sheath–Core Graphite/Silk Fiber Made by Dry-Meyer-Rod-Coating for Wearable Strain Sensors. *ACS Appl. Mater. Interfaces* **2016**, *8*, 20894–20899. [CrossRef]

245. Zhang, R.; Deng, H.; Valenca, R.; Jin, J.; Fu, Q.; Bilotti, E.; Peijs, T. Carbon nanotube polymer coatings for textile yarns with good strain sensing capability. *Sens. Actuators A Phys.* **2012**, *179*, 83–91. [CrossRef]

246. Kowalczyk, D.; Brzezinski, S.; Kaminska, I.; Wrobel, S.; Mizerska, U.; Fortuniak, W.; Piorkowska, E.; Svyntkivska, M.; Makowski, T. Electrically conductive composite textiles modified with graphene using sol-gel method. *J. Alloy. Compd.* **2019**, *784*, 22–28. [CrossRef]

247. Zhang, Y.; Tian, W.; Liu, L.; Cheng, W.; Wang, W.; Liew, K.M.; Wang, B.; Hu, Y. Eco-friendly flame retardant and electromagnetic interference shielding cotton fabrics with multi-layered coatings. *Chem. Eng. J.* **2019**, *372*, 1077–1090. [CrossRef]

248. Shim, E. Coating and laminating processes and techniques for textiles. In *Smart Textile Coatings and Laminates*; Elsevier: Cambridge, UK, 2019; pp. 11–45. [CrossRef]

249. Yang, K.; Torah, R.; Wei, Y.; Beeby, S.; Tudor, J. Waterproof and durable screen printed silver conductive tracks on textiles. *Text. Res. J.* **2013**, *83*, 2023–2031. [CrossRef]

250. Paul, G.; Torah, R.; Yang, K.; Beeby, S.; Tudor, J. An investigation into the durability of screen-printed conductive tracks on textiles. *Meas. Sci. Technol.* **2014**, *25*, 025006. [CrossRef]

251. Sadi, S.; Yang, M.; Luo, L.; Cheng, D.; Cai, G.; Wang, X. Direct screen printing of single-faced conductive cotton fabrics for strain sensing, electrical heating and color changing. *Cellulose* **2019**, *26*, 6179–6188. [CrossRef]

252. Stempien, Z.; Rybicki, E.; Lesnikowski, J. Inkjet-printing deposition of silver electro-conductive layers on textile substrates at low sintering temperature by using an aqueous silver ions-containing ink for textronic applications. *Sens. Actuators B Chem.* **2016**, *224*, 714–725. [CrossRef]

253. Zhou, L.; Fu, J.; He, Y. A Review of 3D Printing Technologies for Soft Polymer Materials. *Adv. Funct. Mater.* **2020**, *30*, 2000187. [CrossRef]

254. Tadesse, M.G.; Dumitrescu, D.; Loghin, C.; Chen, Y.; Wang, L.; Nierstrasz, V. 3D printing of NinjaFlex filament onto PEDOT: PSS-coated textile fabrics for electroluminescence applications. *J. Electron. Mater.* **2018**, *47*, 2082–2092. [CrossRef]

255. Krebs, F.C. Fabrication and processing of polymer solar cells: A review of printing and coating techniques. *Sol. Energy Mater. Sol. Cells* **2009**, *93*, 394–412. [CrossRef]

256. Virkki, J.; Björninen, T.; Merilampi, S.; Sydänheimo, L.; Ukkonen, L. The effects of recurrent stretching on the performance of electro-textile and screen-printed ultra-high-frequency radio-frequency identification tags. *Text. Res. J.* **2014**, *85*, 294–301. [CrossRef]

257. Yang, Y.-L.; Chuang, M.-C.; Lou, S.-L.; Wang, J. Thick-film textile-based amperometric sensors and biosensors. *Analyst* **2010**, *135*, 1230–1234. [CrossRef]

258. Torah, R.; Wei, Y.; Li, Y.; Yang, K.; Beeby, S.; Tudor, J. Printed textile-based electronic devices. In *Handbook of Smart Textiles*; Springer: Singapore, 2015; pp. 653–687. [CrossRef]

259. Fukuda, K.; Someya, T. Recent Progress in the Development of Printed Thin-Film Transistors and Circuits with High-Resolution Printing Technology. *Adv. Mater.* **2016**, *29*, 1602736. [CrossRef]

260. Matavž, A.; Bobnar, V.; Malič, B. Tailoring Ink–Substrate Interactions via Thin Polymeric Layers for High-Resolution Printing. *Langmuir* **2017**, *33*, 11893–11900. [CrossRef] [PubMed]

261. Singh, M.; Haverinen, H.M.; Dhagat, P.; Jabbour, G.E. Inkjet Printing-Process and Its Applications. *Adv. Mater.* **2010**, *22*, 673–685. [CrossRef] [PubMed]

262. Lim, J.A.; Lee, W.H.; Lee, H.S.; Lee, J.H.; Park, Y.D.; Cho, K. Self-Organization of Ink-jet-Printed Triisopropylsilylethynyl Pentacene via Evaporation-Induced Flows in a Drying Droplet. *Adv. Funct. Mater.* **2008**, *18*, 229–234. [CrossRef]

263. Kim, I.; Shahariar, H.; Ingram, W.F.; Zhou, Y.; Jur, J.S. Inkjet Process for Conductive Patterning on Textiles: Maintaining Inherent Stretchability and Breathability in Knit Structures. *Adv. Funct. Mater.* **2018**, *29*, 1807573. [CrossRef]

264. Søndergaard, R.R.; Hösel, M.; Krebs, F.C. Roll-to-Roll fabrication of large area functional organic materials. *J. Polym. Sci. Part B Polym. Phys.* **2012**, *51*, 16–34. [CrossRef]

265. Karim, N.; Afroj, S.; Malandraki, A.; Butterworth, S.; Beach, C.; Rigout, M.; Novoselov, K.S.; Casson, A.J.; Yeates, S.G. All inkjet-printed graphene-based conductive patterns for wearable e-textile applications. *J. Mater. Chem. C* **2017**, *5*, 11640–11648. [CrossRef]

266. Beecroft, M. 3D printing of weft knitted textile based structures by selective laser sintering of nylon powder. *IOP Conf. Ser. Mater. Sci. Eng.* **2016**, *137*, 012017. [CrossRef]

267. Hamzah, H.H.; Shafiee, S.A.; Abdalla, A.; Patel, B.A. 3D printable conductive materials for the fabrication of electrochemical sensors: A mini review. *Electrochem. Commun.* **2018**, *96*, 27–31. [CrossRef]

268. Dip, T.M.; Emu, A.S.; Nafiz, M.N.H.; Kundu, P.; Rakhi, H.R.; Sayam, A.; Akhtarujjman, M.; Shoaib, M.; Ahmed, M.S.; Ushno, S.T.; et al. 3D printing technology for textiles and fashion. *Text. Prog.* **2021**, *52*, 167–260. [CrossRef]

269. Chizari, K.; Daoud, M.A.; Ravindran, A.R.; Therriault, D. 3D Printing of Highly Conductive Nanocomposites for the Functional Optimization of Liquid Sensors. *Small* **2016**, *12*, 6076–6082. [CrossRef]

270. Ambrosi, A.; Moo, J.G.S.; Pumera, M. Helical 3D-Printed Metal Electrodes as Custom-Shaped 3D Platform for Electrochemical Devices. *Adv. Funct. Mater.* **2015**, *26*, 698–703. [CrossRef]

271. Gnanasekaran, K.; Heijmans, T.; van Bennekom, S.; Woldhuis, H.; Wijnia, S.; de With, G.; Friedrich, H. 3D printing of CNT- and graphene-based conductive polymer nanocomposites by fused deposition modeling. *Appl. Mater. Today* **2017**, *9*, 21–28. [CrossRef]

272. Gao, T.; Yang, Z.; Chen, C.; Li, Y.; Fu, K.; Dai, J.; Hitz, E.M.; Xie, H.; Liu, B.; Song, J.; et al. Three-Dimensional Printed Thermal Regulation Textiles. *ACS Nano* **2017**, *11*, 11513–11520. [CrossRef] [PubMed]

273. He, H.; Akbari, M.; Sydänheimo, L.; Ukkonen, L.; Virkki, J. 3D-Printed Graphene Antennas and Interconnections for Textile RFID Tags: Fabrication and Reliability towards Humidity. *Int. J. Antennas Propag.* **2017**, *2017*, 1–5. [CrossRef]

274. Sato, K.; Yamaura, M.; Hagiwara, T.; Murata, K.; Takumoto, M. Study on the electrical conduction mechanism of polypyrrole films. *Synth. Met.* **1991**, *40*, 35–48. [CrossRef]

275. Abthagir, P.; Saraswathi, R. Charge transport and thermal properties of polyindole, polycarbazole and their derivatives. *Thermochim. Acta* **2004**, *424*, 25–35. [CrossRef]

276. Gasana, E.; Westbroek, P.; Hakuzimana, J.; De Clerck, K.; Priniotakis, G.; Kiekens, P.; Tseles, D. Electroconductive textile structures through electroless deposition of polypyrrole and copper at polyaramide surfaces. *Surf. Coat. Technol.* **2006**, *201*, 3547–3551. [CrossRef]

277. Long, Y.; Duvail, J.; Li, M.; Gu, C.; Liu, Z.; Ringer, S.P. Electrical Conductivity Studies on Individual Conjugated Polymer Nanowires: Two-Probe and Four-Probe Results. *Nanoscale Res. Lett.* **2009**, *5*, 237–242. [CrossRef]

278. Rubežienė, V.; Varnaitė-Žuravliova, S. EMI shielding textile materials. In *Materials for Potential EMI Shielding Applications*; Elsevier: Amsterdam, The Netherlands, 2020; pp. 357–378. [CrossRef]

279. Celozzi, S.; Araneo, R.; Lovat, G. *Electromagnetic Shielding*; John Wiley & Sons: New York, NJ, USA, 2008; Volume 192.

280. Cheng, K.B. Production and electromagnetic shielding effectiveness of the knitted stainless steel/polyester fabrics. *J. Text. Engr.* **2000**, *46*, 42–52. [CrossRef]

281. Geetha, S.; Kumar, K.K.S.; Rao, C.R.K.; Vijayan, M.; Trivedi, D.C.K. EMI shielding: Methods and materials-A review. *J. Appl. Polym. Sci.* **2009**, *112*, 2073–2086. [CrossRef]

282. Bagavathi, M.; Priyadarshini, R. A review on the production methods and testing of textiles for electro magnetic interference (EMI) shielding. *Int. J. Eng. Res. Appl.* **2015**, *5*, 2248–9622.

283. Tong, X.C. *Advanced Materials and Design for Electromagnetic Interference Shielding*, 1st ed.; CRC Press: Boca Raton, FL, USA, 2009.

284. Tao, Y.; Li, P.; Shi, S.Q. Effects of Carbonization Temperature and Component Ratio on Electromagnetic Interference Shielding Effectiveness of Woodceramics. *Materials* **2016**, *9*, 540. [CrossRef] [PubMed]

285. Fu, K.K.; Padbury, R.; Toprakci, O.; Dirican, M.; Zhang, X. Conductive textiles. In *Engineering of High-Performance Textiles*; Woodhead Publishing: Cambridge, UK, 2018; pp. 305–334. [CrossRef]

286. Tezel, S.; Kavuşturan, Y.; Vandenbosch, G.A.; Volski, V. Comparison of electromagnetic shielding effectiveness of conductive single jersey fabrics with coaxial transmission line and free space measurement techniques. *Text. Res. J.* **2013**, *84*, 461–476. [CrossRef]

287. Hassan, Z.; Kalaoglu, F.; Atalay, O. Development and characterization of conductive textile (cotton) for wearable electronics and soft robotic applications. *Text. Res. J.* **2020**, *90*, 1792–1804. [CrossRef]

288. Gonçalves, C.; da Silva, A.F.; Gomes, J.; Simoes, R. Wearable E-Textile Technologies: A Review on Sensors, Actuators and Control Elements. *Inventions* **2018**, *3*, 14. [CrossRef]

289. Fishlock, D. A panacea for all bodily ills. *IEE Rev.* **2001**, 23–28. [CrossRef]

290. Thorp, E. The invention of the first wearable computer. In Proceedings of the Digest of Papers. Second International Symposium on Wearable Computers (Cat. No.98EX215), Pittsburgh, PA, USA, 19–20 October 1998; pp. 4–8. [CrossRef]

291. Gopalsamy, C.; Park, S.; Rajamanickam, R.; Jayaraman, S. The Wearable Motherboard?: The first generation of adaptive and responsive textile structures (ARTS) for medical applications. *Virtual Real.* **1999**, *4*, 152–168. [CrossRef]

292. Paradiso, R.; Loriga, G.; Taccini, N.; Gemignani, A.; Ghelarducci, B. WEALTHY-a wearable healthcare system: New frontier on e-textile. *J. Telecommun. Inf. Technol.* **2005**, *4*, 105–113.

293. Pirotte, F.; Depré, A.; Shishoo, R.; De Jonckheere, J.; Grillet, A. Smart textiles embedded with optical fibre sensors for health monitoring of patients. In *Medical and Healthcare Textiles*; Woodhead Publishing: Cambridge, UK, 2010; pp. 463–471. [CrossRef]

294. Asada, H.H.; Shaltis, P.; Mccombie, D.B.; Reisner, A.T. Wearable Blood Pressure Sensor and Method of Calibration. U.S. Patent 7,641,614 B2, 5 January 2010.

295. Teng, X.-F.; Zhang, Y.-T.; Poon, C.C.Y.; Bonato, P. Wearable Medical Systems for p-Health. *IEEE Rev. Biomed. Eng.* **2008**, *1*, 62–74. [CrossRef]

296. Edmison, J.; Jones, M.; Lockhart, T.; Martin, T. An e-textile system for motion analysis. *Stud. Health Technol. Inform.* **2004**, *108*, 292–301.

297. Enokibori, Y.; Ito, Y.; Suzuki, A.; Mizuno, H.; Shimakami, Y.; Kawabe, T.; Mase, K. SpiroVest: An e-textile-based wearable spirometer with posture change adaptability. In Proceedings of the 2013 ACM Conference on Pervasive and Ubiquitous Computing Adjunct Publication, Zurich, Switzerland, 8–12 September 2013; pp. 203–206. [CrossRef]

298. Enokibori, Y.; Mase, K. Human joint angle estimation with an e-textile sensor. In Proceedings of the 2014 ACM International Symposium on Wearable Computers, Seattle, WA, USA, 13–17 September 2014; pp. 129–130. [CrossRef]

299. Yapici, M.K.; Alkhidir, T.E. Intelligent Medical Garments with Graphene-Functionalized Smart-Cloth ECG Sensors. *Sensors* **2017**, *17*, 875. [CrossRef] [PubMed]

300. Lin, Z.; Yang, J.; Li, X.; Wu, Y.; Wei, W.; Liu, J.; Chen, J.; Yang, J. Large-Scale and Washable Smart Textiles Based on Triboelectric Nanogenerator Arrays for Self-Powered Sleeping Monitoring. *Adv. Funct. Mater.* **2017**, *28*, 1704112. [CrossRef]

301. Li, X.; Koh, K.H.; Farhan, M.; Lai, K.W.C. An ultraflexible polyurethane yarn-based wearable strain sensor with a polydimethyl-siloxane infiltrated multilayer sheath for smart textiles. *Nanoscale* **2020**, *12*, 4110–4118. [CrossRef]

302. Chen, G.; Zhao, X.; Andalib, S.; Xu, J.; Zhou, Y.; Tat, T.; Lin, K.; Chen, J. Discovering giant magnetoelasticity in soft matter for electronic textiles. *Matter* **2021**, *4*, 3725–3740. [CrossRef]

303. Castano, L.M.; Flatau, A.B. Smart fabric sensors and e-textile technologies: A review. *Smart Mater. Struct.* **2014**, *23*, 053001. [CrossRef]

304. Fleury, A.; Sugar, M.; Chau, T. E-textiles in Clinical Rehabilitation: A Scoping Review. *Electronics* **2015**, *4*, 173–203. [CrossRef]

305. Tsukada, Y.T.; Tokita, M.; Murata, H.; Hirasawa, Y.; Yodogawa, K.; Iwasaki, Y.-K.; Asai, K.; Shimizu, W.; Nakashima, H.; Tsukada, S. Validation of wearable textile electrodes for ECG monitoring. *Heart Vessel.* **2019**, *34*, 1203–1211. [CrossRef] [PubMed]

306. Stoppa, M.; Chiolerio, A. Wearable electronics and smart textiles: A critical review. *Sensors* **2014**, *14*, 11957–11992. [CrossRef]

307. Esfahani, M.I.M. Smart textiles in healthcare: A summary of history, types, applications, challenges, and future trends. In *Nanosensors and Nanodevices for Smart Multifunctional Textiles*; Elsevier: Amsterdam, The Netherlands, 2020; pp. 93–107. [CrossRef]

308. Axisa, F.; Schmitt, P.; Gehin, C.; Delhomme, G.; McAdams, E.; Dittmar, A. Flexible Technologies and Smart Clothing for Citizen Medicine, Home Healthcare, and Disease Prevention. *IEEE Trans. Inf. Technol. Biomed.* **2005**, *9*, 325–336. [CrossRef]

309. Shishoo, R. *Textiles in Sport*, 1st ed.; Elsevier: Cambridge, UK, 2005.

310. Munro, B.J.; Campbell, T.E.; Wallace, G.G.; Steele, J.R. The intelligent knee sleeve: A wearable biofeedback device. *Sens. Actuators B Chem.* **2008**, *131*, 541–547. [CrossRef]

311. Casa, D.J.; Armstrong, L.E.; Hillman, S.K.; Montain, S.J.; Reiff, R.V.; Rich, B.S.E.; Roberts, W.O.; Stone, J.A. National athletic trainers' association position statement: Fluid replacement for athletes. *J. Athl. Train.* **2000**, *35*, 212–224. [PubMed]

312. Morris, D.; Schazmann, B.; Wu, Y.; Coyle, S.; Brady, S.; Hayes, J.; Slater, C.; Fay, C.; Lau, K.T.; Wallace, G.; et al. Wearable sensors for monitoring sports performance and training. In Proceedings of the 2008 5th International Summer School and Symposium on Medical Devices and Biosensors, Hong Kong, China, 1–3 June 2008; pp. 121–124. [CrossRef]

313. Seyedin, S.; Razal, J.M.; Innis, P.C.; Jeiranikhameneh, A.; Beirne, S.; Wallace, G.G. Knitted Strain Sensor Textiles of Highly Conductive All-Polymeric Fibers. *ACS Appl. Mater. Interfaces* **2015**, *7*, 21150–21158. [CrossRef] [PubMed]

314. Hu, X.; Tian, M.; Xu, T.; Sun, X.; Sun, B.; Sun, C.; Liu, X.; Zhang, X.; Qu, L. Multiscale Disordered Porous Fibers for Self-Sensing and Self-Cooling Integrated Smart Sportswear. *ACS Nano* **2019**, *14*, 559–567. [CrossRef] [PubMed]

315. Rus, D.; Tolley, M.T. Design, fabrication and control of soft robots. *Nature* **2015**, *521*, 467–475. [CrossRef]

316. Wang, H.; Totaro, M.; Beccai, L. Toward Perceptive Soft Robots: Progress and Challenges. *Adv. Sci.* **2018**, *5*, 1800541. [CrossRef]

317. Xiong, J.; Chen, J.; Lee, P.S. Functional Fibers and Fabrics for Soft Robotics, Wearables, and Human–Robot Interface. *Adv. Mater.* **2020**, *33*, e2002640. [CrossRef]

318. Furuse, A.; Hashimoto, M. Development of novel textile and yarn actuators using plasticized PVC gel. In Proceedings of the Electroactive Polymer Actuators and Devices (EAPAD) 2017, Portland, OR, USA, 25–29 March 2017; Volume 10163, p. 1016327. [CrossRef]

319. Guo, J.; Xiang, C.; Helps, T.; Taghavi, M.; Rossiter, J. Electroactive textile actuators for wearable and soft robots. In Proceedings of the 2018 IEEE International Conference on Soft Robotics (RoboSoft), Livorno, Italy, 24–28 April 2018; pp. 339–343. [CrossRef]

320. Cianchetti, M.; Renda, F.; Licofonte, A.; Laschi, C. Sensorization of continuum soft robots for reconstructing their spatial configuration. In Proceedings of the 2012 4th IEEE RAS & EMBS International Conference on Biomedical Robotics and Biomechatronics (BioRob), Rome, Italy, 24–27 June 2012; pp. 634–639. [CrossRef]

321. Atalay, A.; Sanchez, V.; Atalay, O.; Vogt, D.M.; Haufe, F.; Wood, R.J.; Walsh, C.J. Batch Fabrication of Customizable Silicone-Textile Composite Capacitive Strain Sensors for Human Motion Tracking. *Adv. Mater. Technol.* **2017**, *2*, 1700136. [CrossRef]

322. Kanik, M.; Orguc, S.; Varnavides, G.; Kim, J.; Benavides, T.; Gonzalez, D.; Akintilo, T.; Tasan, C.C.; Chandrakasan, A.P.; Fink, Y.; et al. Strain-programmable fiber-based artificial muscle. *Science* **2019**, *365*, 145–150. [CrossRef]

323. Pei, Z.; Xiong, X.; He, J.; Zhang, Y. Highly Stretchable and Durable Conductive Knitted Fabrics for the Skins of Soft Robots. *Soft Robot.* **2019**, *6*, 687–700. [CrossRef]

324. Nashed, M.-N.; Hardy, D.A.; Hughes-Riley, T.; Dias, T. A Novel Method for Embedding Semiconductor Dies within Textile Yarn to Create Electronic Textiles. *Fibers* **2019**, *7*, 12. [CrossRef]

325. Lian, Y.; Yu, H.; Wang, M.; Yang, X.; Li, Z.; Yang, F.; Wang, Y.; Tai, H.; Liao, Y.; Wu, J.; et al. A multifunctional wearable E-textile via integrated nanowire-coated fabrics. *J. Mater. Chem. C* **2020**, *8*, 8399–8409. [CrossRef]

326. Poupyrev, I.; Gong, N.-W.; Fukuhara, S.; Karagozler, M.E.; Schwesig, C.; Robinson, K.E. Project Jacquard: Interactive digital textiles at scale. In Proceedings of the 2016 CHI Conference on Human Factors in Computing Systems, San Jose, CA, USA, 7–12 May 2016; pp. 4216–4227. [CrossRef]

327. Australian Radiation Protection and Nuclear Safety Agency. Mobile Phones and Health. Available online: https://www.arpansa.gov.au/understanding-radiation/radiation-sources/more-radiation-sources/mobile-phones?fbclid=IwAR3M-JEZTmbLZExqYD0C8YcFq23l-EsQH3pfYys-hyn4fUUkdrFhorJdaHo (accessed on 14 January 2022).

328. International Commission on Non-Ionizing Radiation. Guidelines for limiting exposure to time-varying electric, magnetic, and electromagnetic fields (up to 300 GHz). *Health Phys.* **1998**, *74*, 494–521.

329. Hirata, A.; Matsuyama, S.-I.; Shiozawa, T. Temperature rises in the human eye exposed to EM waves in the frequency range 0.6–6 GHz. *IEEE Trans. Electromagn. Compat.* **2000**, *42*, 386–393. [CrossRef]

330. Mille, M.W. Electrical Wiring Configurations and Childhood Cancer. Volume 112. 1980. Available online: https://www.osti.gov/biblio/7055661 (accessed on 14 January 2022).

331. Wdowiak, A.; Mazurek, P.; Wdowiak, A.; Bojar, I. Effect of electromagnetic waves on human reproduction. *Ann. Agric. Environ. Med.* **2017**, *24*, 13–18. [CrossRef]

332. Zou, L.; Lan, C.; Yang, L.; Xu, Z.; Chu, C.; Liu, Y.; Qiu, Y. The optimization of nanocomposite coating with polyaniline coated carbon nanotubes on fabrics for exceptional electromagnetic interference shielding. *Diam. Relat. Mater.* **2020**, *104*, 107757. [CrossRef]

333. Zhu, S.; Wang, M.; Qiang, Z.; Song, J.; Wang, Y.; Fan, Y.; You, Z.; Liao, Y.; Zhu, M.; Ye, C. Multi-functional and highly conductive textiles with ultra-high durability through 'green' fabrication process. *Chem. Eng. J.* **2020**, *406*, 127140. [CrossRef]

334. Yin, G.; Wang, Y.; Wang, W.; Yu, D. Multilayer structured PANI/MXene/CF fabric for electromagnetic interference shielding constructed by layer-by-layer strategy. *Colloids Surfaces A Physicochem. Eng. Asp.* **2020**, *601*, 125047. [CrossRef]

335. Yin, G.; Wang, Y.; Wang, W.; Qu, Z.; Yu, D. A Flexible Electromagnetic Interference Shielding Fabric Prepared by Construction of PANI/MXene Conductive Network via Layer-by-Layer Assembly. *Adv. Mater. Interfaces* **2021**, *8*, 2001893. [CrossRef]

336. Jia, L.-C.; Ding, K.-Q.; Ma, R.-J.; Wang, H.-L.; Sun, W.-J.; Yan, D.-X.; Li, B.; Li, Z.-M. Highly Conductive and Machine-Washable Textiles for Efficient Electromagnetic Interference Shielding. *Adv. Mater. Technol.* **2018**, *4*, 1800503. [CrossRef]

337. Zong, J.-Y.; Zhou, X.-J.; Hu, Y.-F.; Yang, T.-B.; Yan, D.-X.; Lin, H.; Lei, J.; Li, Z.-M. A wearable multifunctional fabric with excellent electromagnetic interference shielding and passive radiation heating performance. *Compos. Part B Eng.* **2021**, *225*, 109299. [CrossRef]

338. Jia, L.-C.; Xu, L.; Ren, F.; Ren, P.-G.; Yan, D.-X.; Li, Z.-M. Stretchable and durable conductive fabric for ultrahigh performance electromagnetic interference shielding. *Carbon* **2018**, *144*, 101–108. [CrossRef]

339. Ghosh, S.; Ganguly, S.; Das, P.; Das, T.K.; Bose, M.; Singha, N.K.; Das, A.K.; Das, N.C. Fabrication of Reduced Graphene Oxide/Silver Nanoparticles Decorated Conductive Cotton Fabric for High Performing Electromagnetic Interference Shielding and Antibacterial Application. *Fibers Polym.* **2019**, *20*, 1161–1171. [CrossRef]

340. Ghouri, A.S.; Aslam, R.; Siddiqui, M.S.; Sami, S.K. Recent Progress in Textile-Based Flexible Supercapacitor. *Front. Mater.* **2020**, *7*, 58. [CrossRef]

341. Xue, Q.; Sun, J.; Huang, Y.; Zhu, M.; Pei, Z.; Li, H.; Wang, Y.; Li, N.; Zhang, H.; Zhi, C. Recent Progress on Flexible and Wearable Supercapacitors. *Small* **2017**, *13*, 1701827. [CrossRef] [PubMed]

342. Liu, F.; Zeng, L.; Chen, Y.; Zhang, R.; Yang, R.; Pang, J.; Ding, L.; Liu, H.; Zhou, W. Ni-Co-N hybrid porous nanosheets on graphene paper for flexible and editable asymmetric all-solid-state supercapacitors. *Nano Energy* **2019**, *61*, 18–26. [CrossRef]

343. Dai, S.; Xu, W.; Xi, Y.; Wang, M.; Gu, X.; Guo, D.; Hu, C. Charge storage in KCu7S4 as redox active material for a flexible all-solid-state supercapacitor. *Nano Energy* **2016**, *19*, 363–372. [CrossRef]

344. Wang, Z.; Zhu, M.; Pei, Z.; Xue, Q.; Li, H.; Huang, Y.; Zhi, C. Polymers for supercapacitors: Boosting the development of the flexible and wearable energy storage. *Mater. Sci. Eng. R Rep.* **2019**, *139*, 100520. [CrossRef]

345. Ren, M.; Di, J.; Chen, W. Recent Progress and Application Challenges of Wearable Supercapacitors. *Batter. Supercaps.* **2021**, *4*, 1279–1290. [CrossRef]

346. Song, P.; He, X.; Xie, M.; Tao, J.; Shen, X.; Ji, Z.; Yan, Z.; Zhai, L.; Yuan, A. Polyaniline wrapped graphene functionalized textile with ultrahigh areal capacitance and energy density for high-performance all-solid-state supercapacitors for wearable electronics. *Compos. Sci. Technol.* **2020**, *198*, 108305. [CrossRef]

347. Kim, T.; Samuel, E.P.; Park, C.; Kim, Y.-I.; Aldalbahi, A.; Alotaibi, F.; Yoon, S.S. Wearable fabric supercapacitors using supersonically sprayed reduced graphene and tin oxide. *J. Alloy. Compd.* **2020**, *856*, 157902. [CrossRef]

348. Lu, C.; Wang, D.; Zhao, J.; Han, S.; Chen, W. A Continuous Carbon Nitride Polyhedron Assembly for High-Performance Flexible Supercapacitors. *Adv. Funct. Mater.* **2017**, *27*, 1606219. [CrossRef]

349. Lv, Z.; Luo, Y.; Tang, Y.; Wei, J.; Zhu, Z.; Zhou, X.; Li, W.; Zeng, Y.; Zhang, W.; Zhang, Y.; et al. Editable Supercapacitors with Customizable Stretchability Based on Mechanically Strengthened Ultralong $MnO_2$ Nanowire Composite. *Adv. Mater.* **2017**, *30*, 1704531. [CrossRef] [PubMed]

350. Wagner, S.; Bonderover, E.; Jordan, W.B.; Sturm, J.C. Electrotextiles: Concepts and challenges. *Int. J. High Speed Electron. Syst.* **2002**, *12*, 391–399. [CrossRef]

351. Islam, G.M.N.; Ali, M.A.; Collie, S. Textile sensors for wearable applications: A comprehensive review. *Cellulose* **2020**, *27*, 6103–6131. [CrossRef]

352. Badghaish, H.S.; Hussain, M.M. Textile Electronics–Prospects, Advances, Challenges and Opportunities. *MRS Adv.* **2020**, *5*, 2359–2379. [CrossRef]

353. Molla, T.I.; Compton, C.; Dunne, L.E. Identifying Challenges of Fabricating E-textile Garments Via a Case Study. In Proceedings of the International Textile and Apparel Association Annual Conference Proceedings, Las Vegas, NV, USA, 25–29 October 2019; Volume 76. [CrossRef]

354. Gao, Y.; Xie, C.; Zheng, Z. Textile Composite Electrodes for Flexible Batteries and Supercapacitors: Opportunities and Challenges. *Adv. Energy Mater.* **2020**, *11*, 2002838. [CrossRef]

355. Levitt, A.; Hegh, D.; Phillips, P.; Uzun, S.; Anayee, M.; Razal, J.M.; Gogotsi, Y.; Dion, G. 3D knitted energy storage textiles using MXene-coated yarns. *Mater. Today* **2020**, *34*, 17–29. [CrossRef]